The Murchison Widefield Array (MWA)

Gianni Bernardi
Harvard-Smithsonian Center for Astrophysics
(thanks to the whole MWA collaboration and particularly to L. Greenhill, D. Mitchell, S. Ord & R.Wayth)

Relevant digression… WSRT observations of the 3C196 field
(Bernardi et al. 2010, A&A, 522, 67)

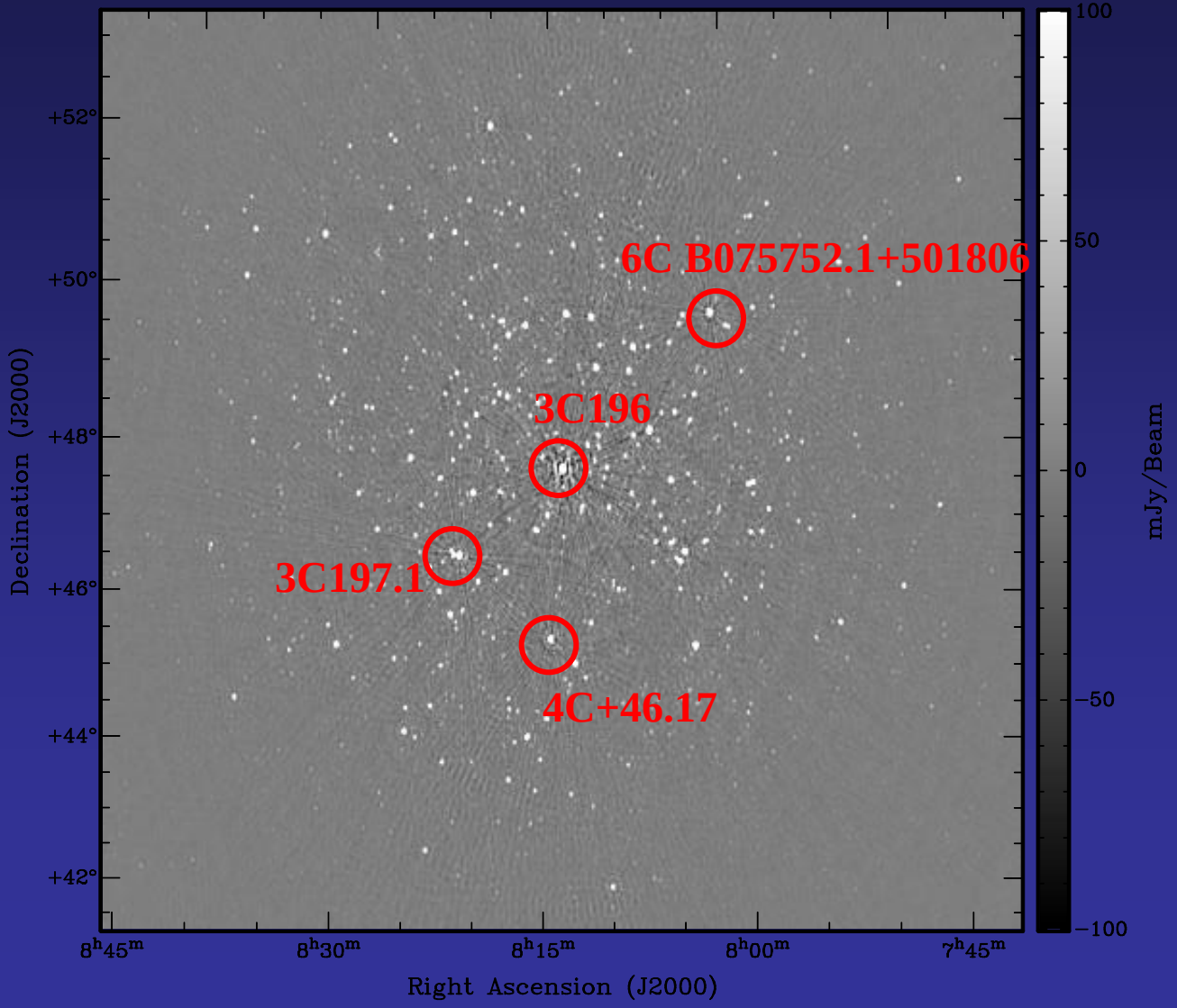

Westerbork image of the 3C196 field at 150 MHz

self-developed Aips++/CASA pipeline

peak flux ~ 77.4 Jy

conversion factor: 1mJy/beam=3.3 K

noise: 0.5 mJy/beam

DDEs in CASA: calibration and peeling

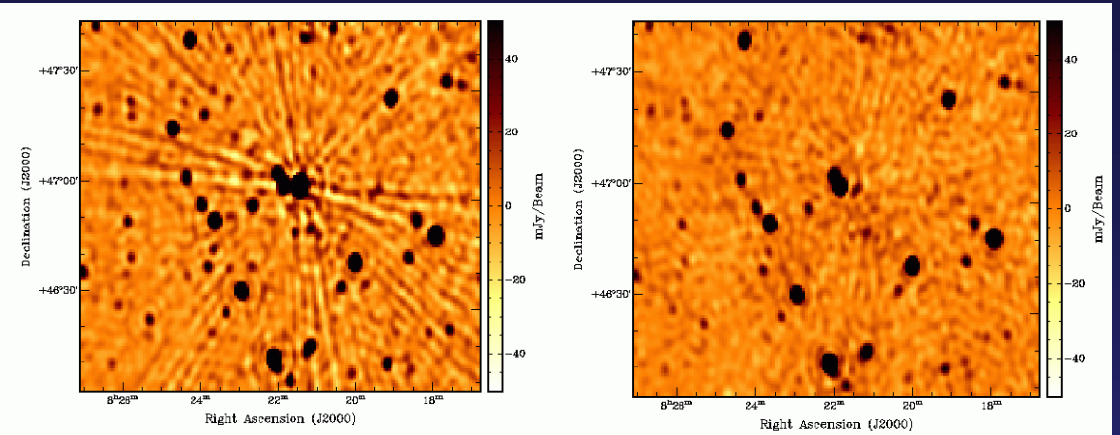

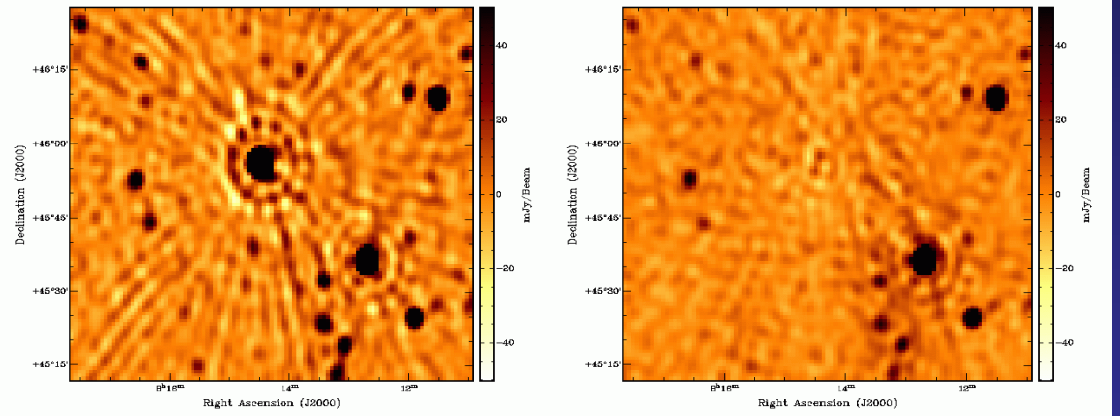

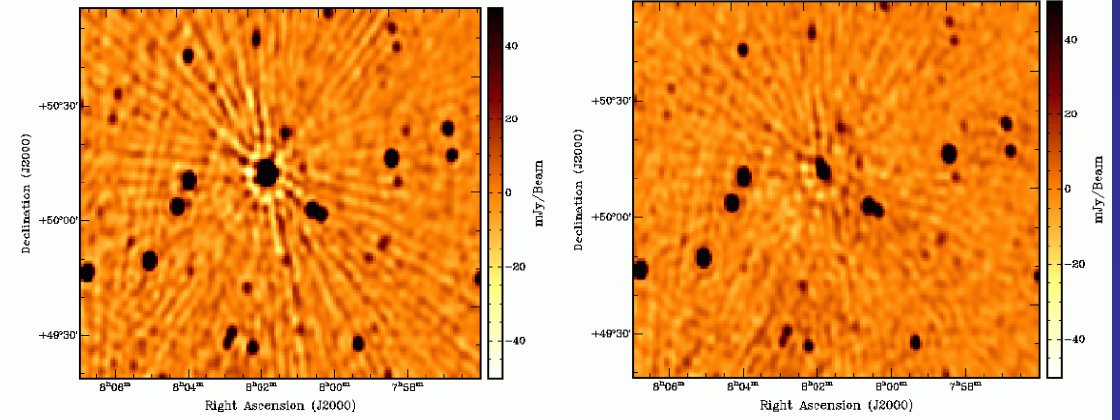

3C197.1: ~6.8 Jy
Solutions every 10 sec after averaging the visibilities over ~230 channels
rms residual: ~9.8 mJy
Calibration accuracy: <0.2%

4C+46.17: ~6.2 Jy
Solutions every 10 sec after averaging the visibilities over ~230 channels
rms residual: ~6.2 mJy
Calibration accuracy: <0.2%

6C B075752.1+501806: ~5.8 Jy
Solutions every 10 sec after averaging the visibilities over ~230 channels
rms residual: ~6.2 mJy
Calibration accuracy: ~0.4%

Residual image: where the EoR science happens!

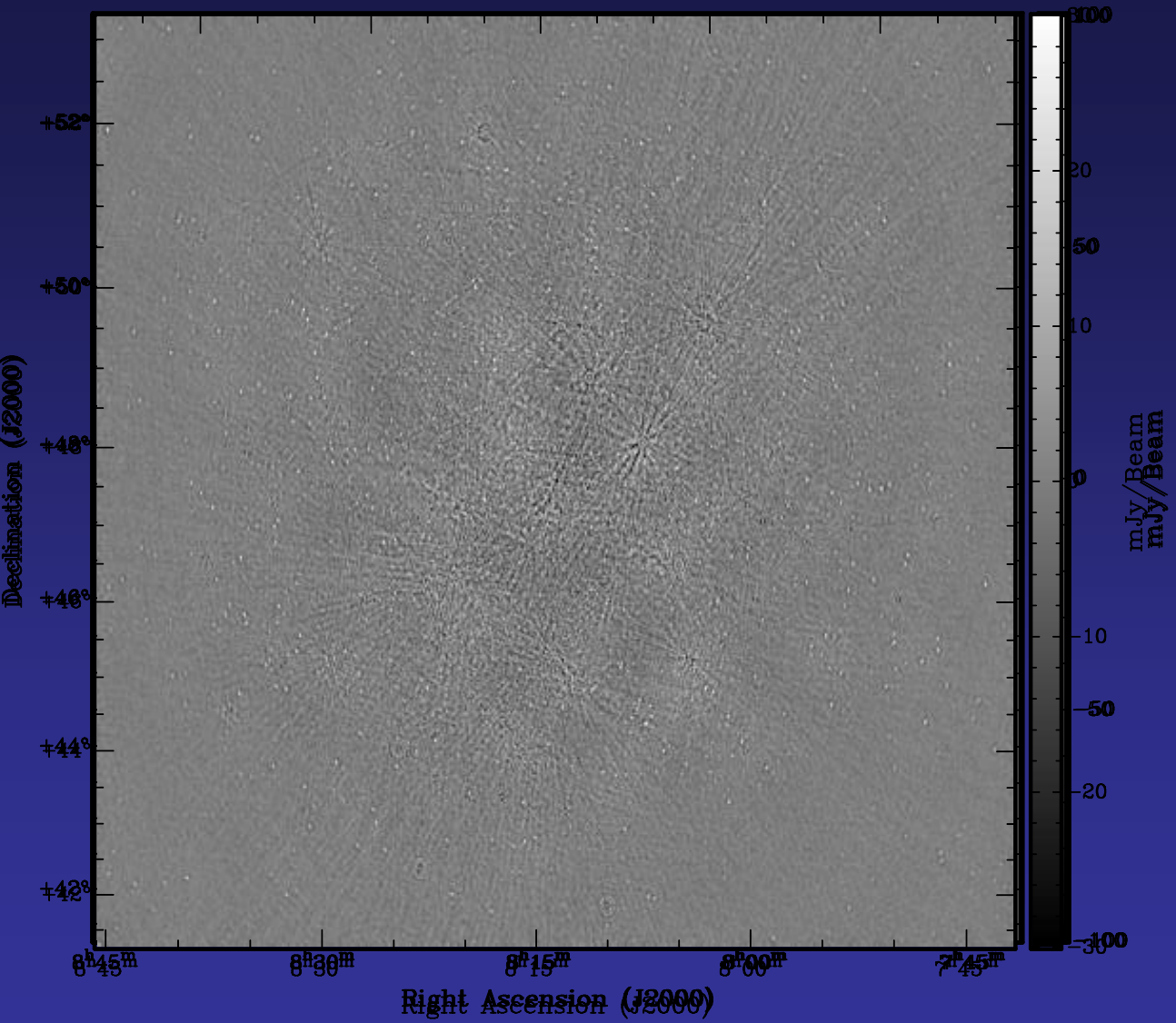

total intensity image after the sources down to 30 mJy were subtracted: some evidence of fluctuations on very large scales (> 30 arcmin) which can be attributed to the Galaxy

Formal dynamic range: 150000:1
Actual dynamic range: 40000:1

WSRT observations of the FAN field

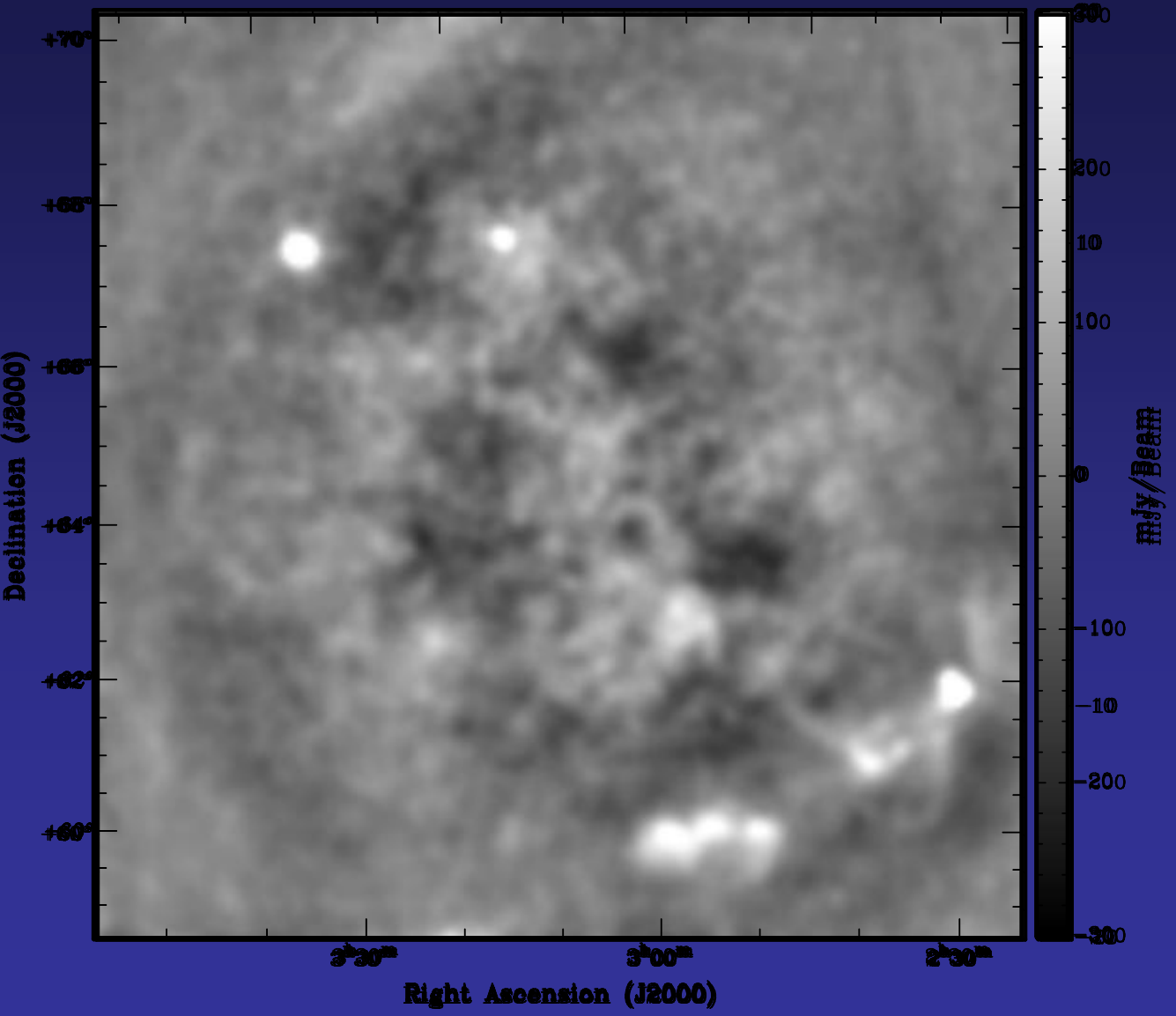

total intensity image obtained by averaging all the spectral bands and six nights of data

average frequency: 150 MHz

peak flux ~ 2.8 Jy

conversion factor: 1mJy/beam=4 K

noise: 0.75 mJy/beam

Power spectrum analysis (4th GC)

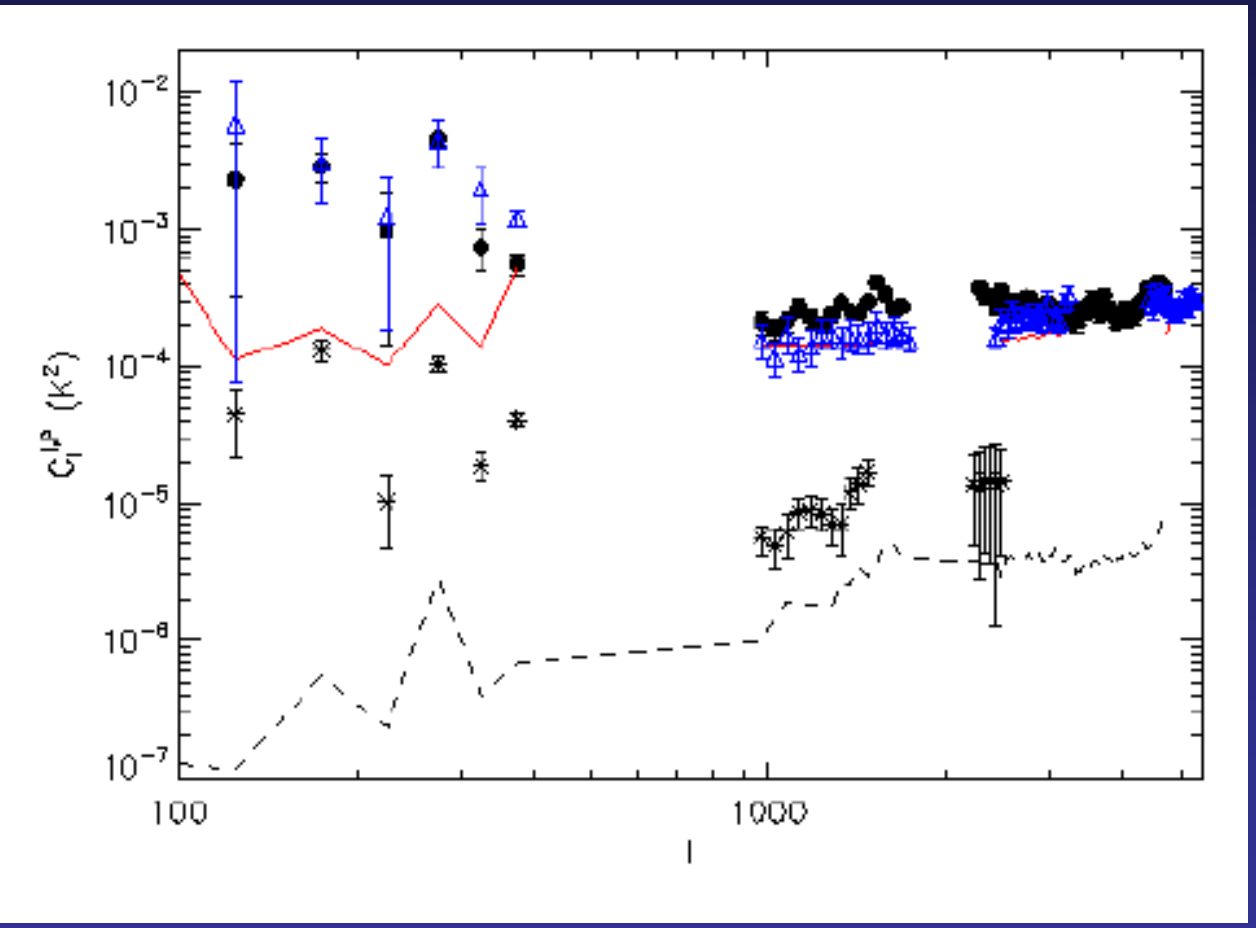

Black circles = 3C196

Blue = NCP

Red line = estimated power spectrum of the confusion noise

Black asterisks = polarization power spectrum of the 3C196 area

Dashed line = power spectrum of the estimated thermal noise

Total intensity *rms* fluctuations on 30': 3.4 ± 0.2 K (3C196), 5.5 ± 0.3 K (NCP)
Polarization *rms* fluctuations on 30': 0.68 ± 0.03 K (3C196)

Current best EoR upper limits

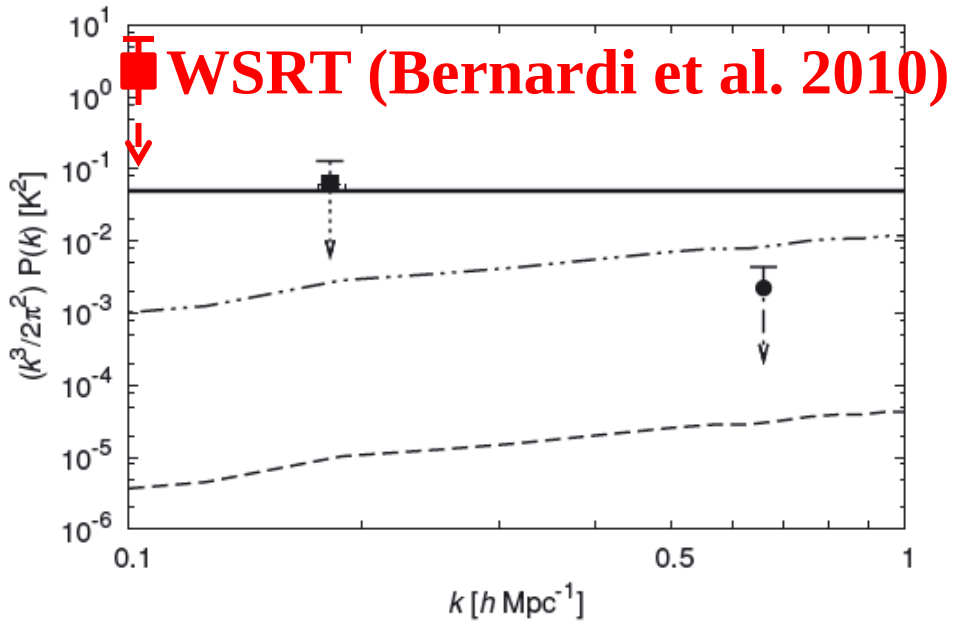

Figure 11. 3D power spectrum for the data shown in Fig. 10, using $k^2 = k_\parallel^2 + k_\perp^2$. This is dominated by $k_\parallel$, so the binwidth in $k_\perp$ does not influence the horizontal position of the limits. The strongest constraints from the 2 and 0.5 MHz filters are shown (square and circle, respectively). Upper limits are 2σ bootstrap errors. Three possible signals are shown. The dashed line is the prediction from Iliev et al. (2008) and the double-dot–dashed line is the same for a cold IGM. The solid line comes from the single-scale bubble model as described in the text for a cold IGM, using $k = 2.5/R$ to show the maximum power at all k. For the two points shown, the bubble diametres which achieve this maximum power are 27 and 7.4 h^{-1} Mpc, respectively. Only the 0.5-MHz point imposes a limit on the diametre. For a warm IGM case, this signal would be reduced by the same factor as in the two dashed lines.

Paciga et al. 2011

MWA Consortium

Australia, India, USA and New Zealand

Curtin University
Australian National University
The University of Sydney
The University of Melbourne
The University of Tasmania
Swinburne University of Technology
The University of Western Australia
CSIRO

Raman Research Institute

Victoria University, Wellington

MIT Haystack Observatory
MIT Kavli Institute
Harvard-Smithsonian CfA
University of Washington
Arizona State University

The Murchison Wide-field Array is an official Square Kilometre Array Precursor (an SKA technology pathfinder on one of the two candidate SKA sites – Western Australia or South Africa).

~$A30M project (funded by US, Australia, India and New Zealand). Buildout and early science phase supported with ~$A12M of Australian and New Zealand cash.

Lonsdale et al. 2009, Proc. IEEE, 97, 1497

Low frequency (80 – 300 MHz: 32 MHz bandwidth), large-N (correlation rich) array. Neutral hydrogen at redshifts of ~5 – 10;

Aperture array antenna elements, 4 x 4 arrays of dual polarisation dipoles – “tiles”;

Initially 128 tiles, expandable to 512;

Wide field of view (15°-30°)

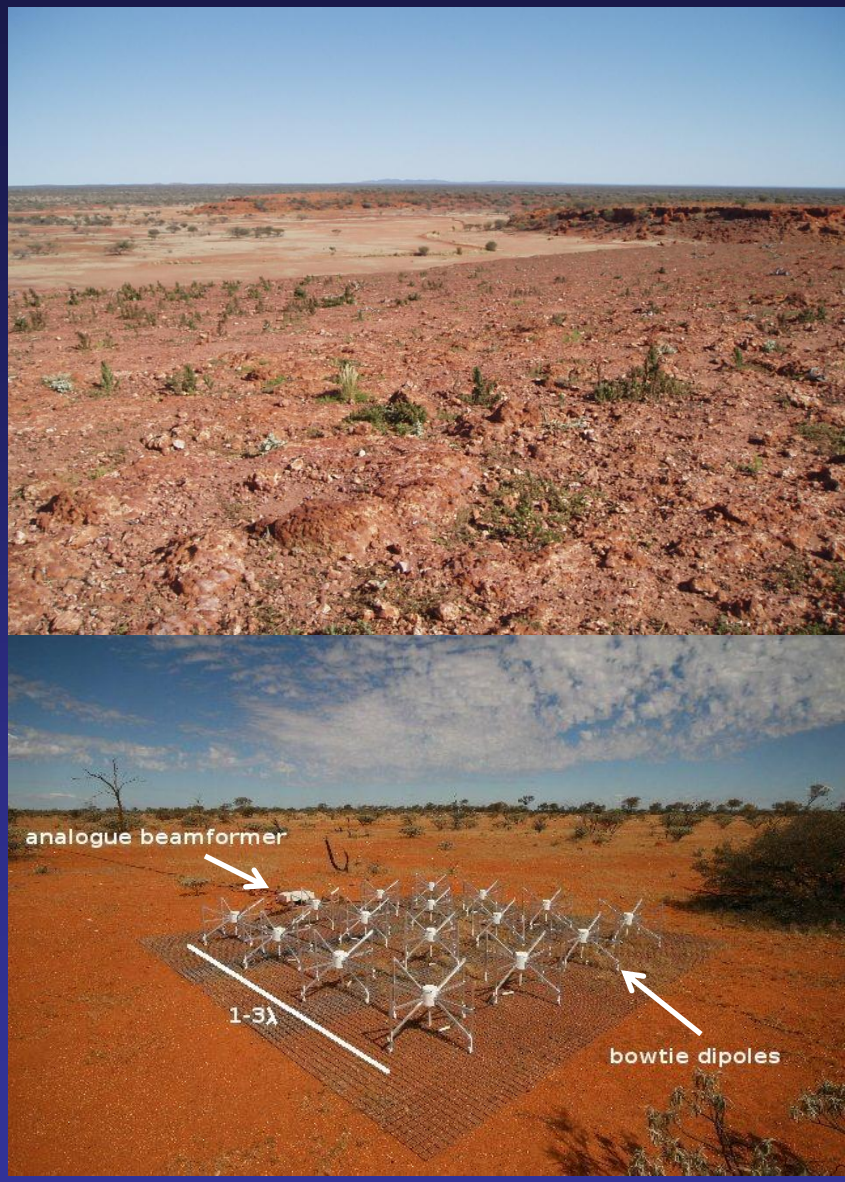

Excellent instantaneous PSF

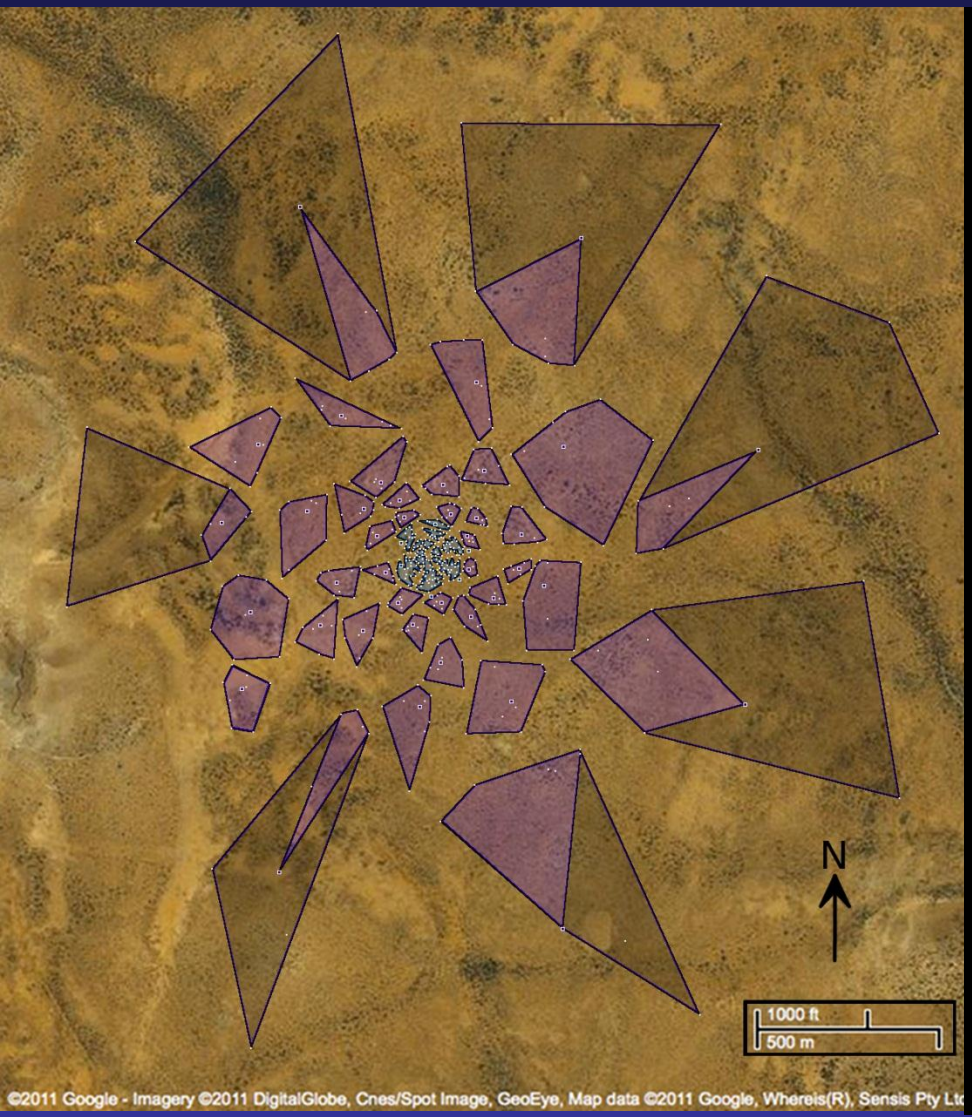

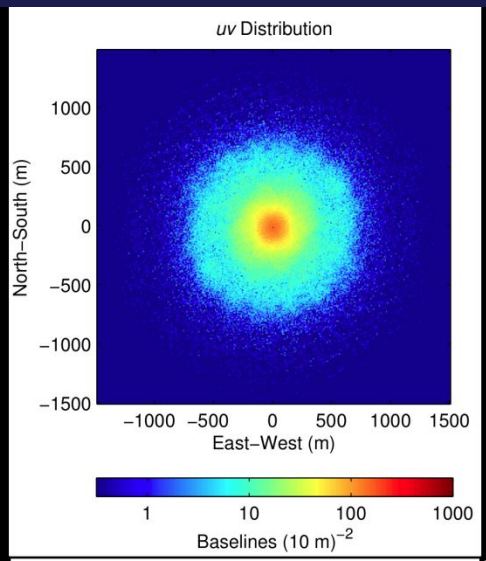

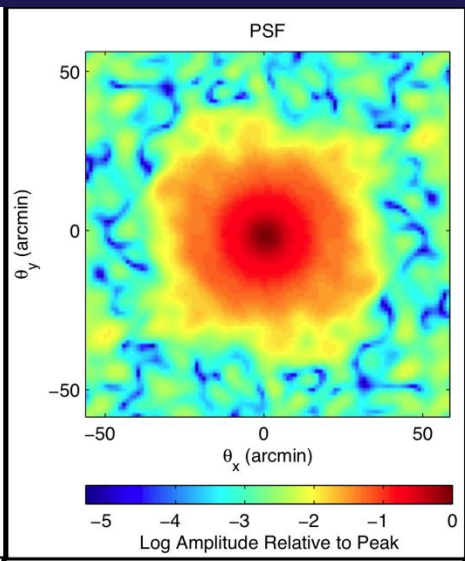

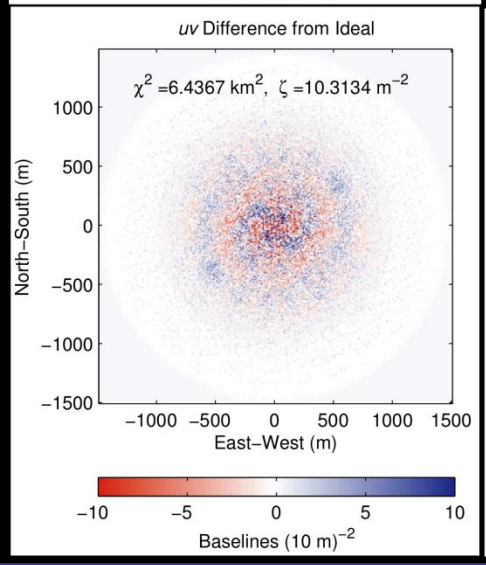

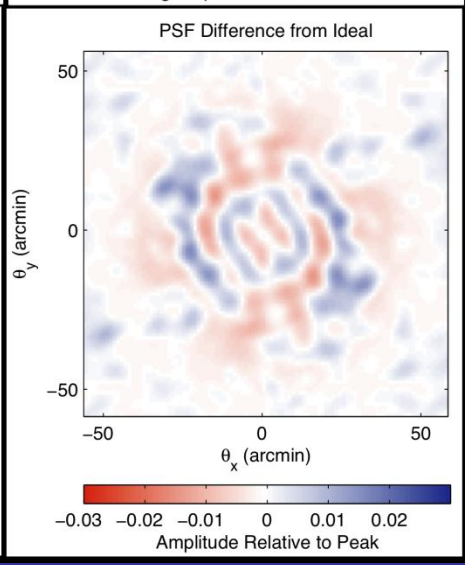


Murchison Shire Boundary
Population Density: 0.002 km^{-2}

Sydney

Pop. 4 million

Narrabri

Pop. 6,000

Boolardy

SKA site

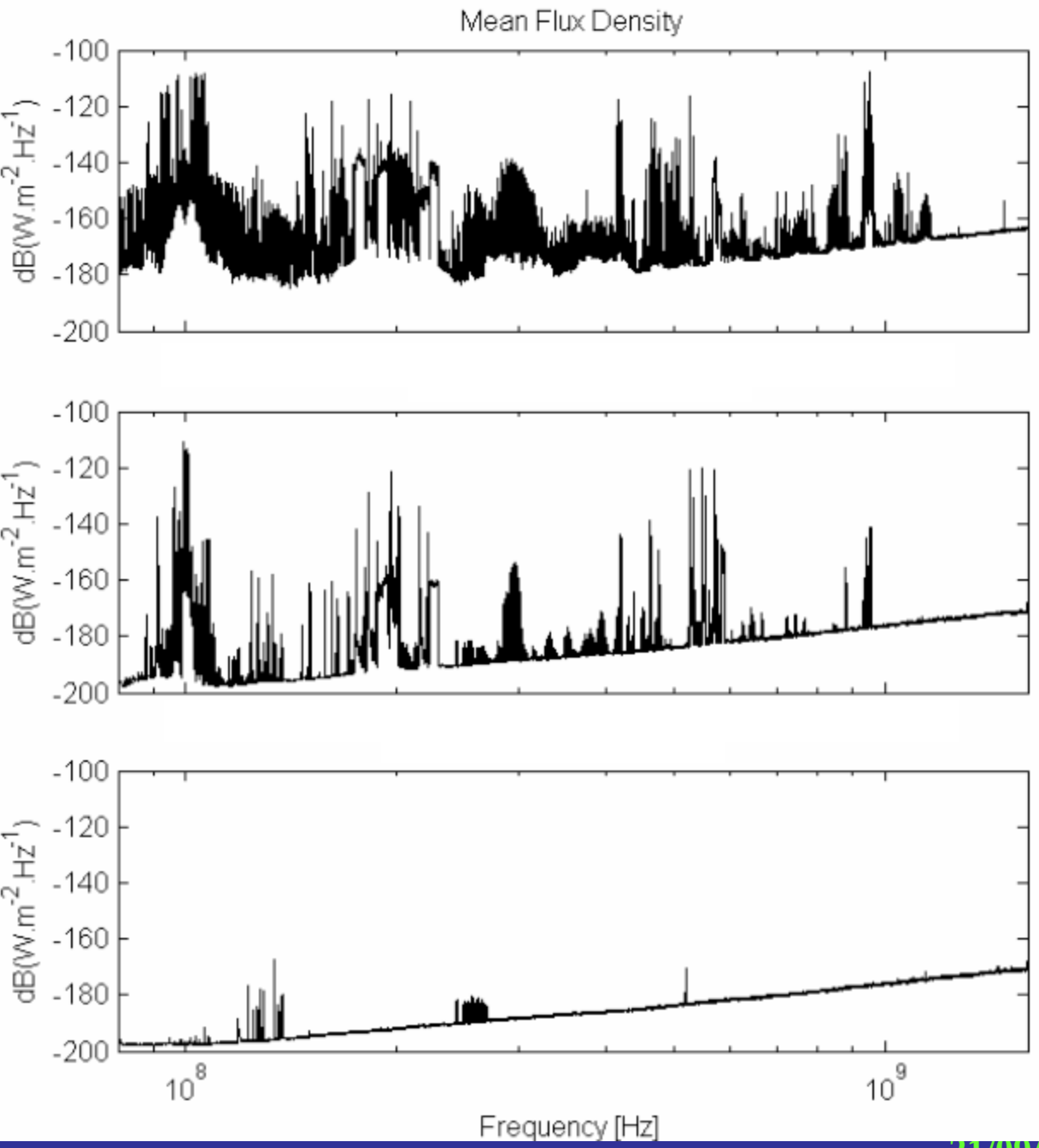

MWA analysis pipeline

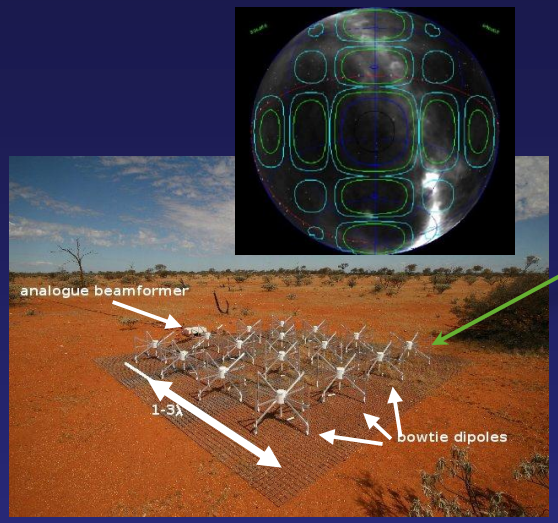

FPGAs

Real-Time System: CPUs/MPI + GPUs

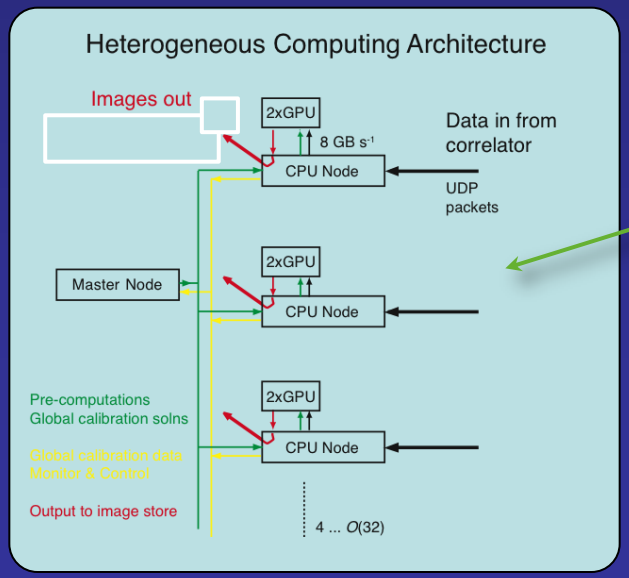

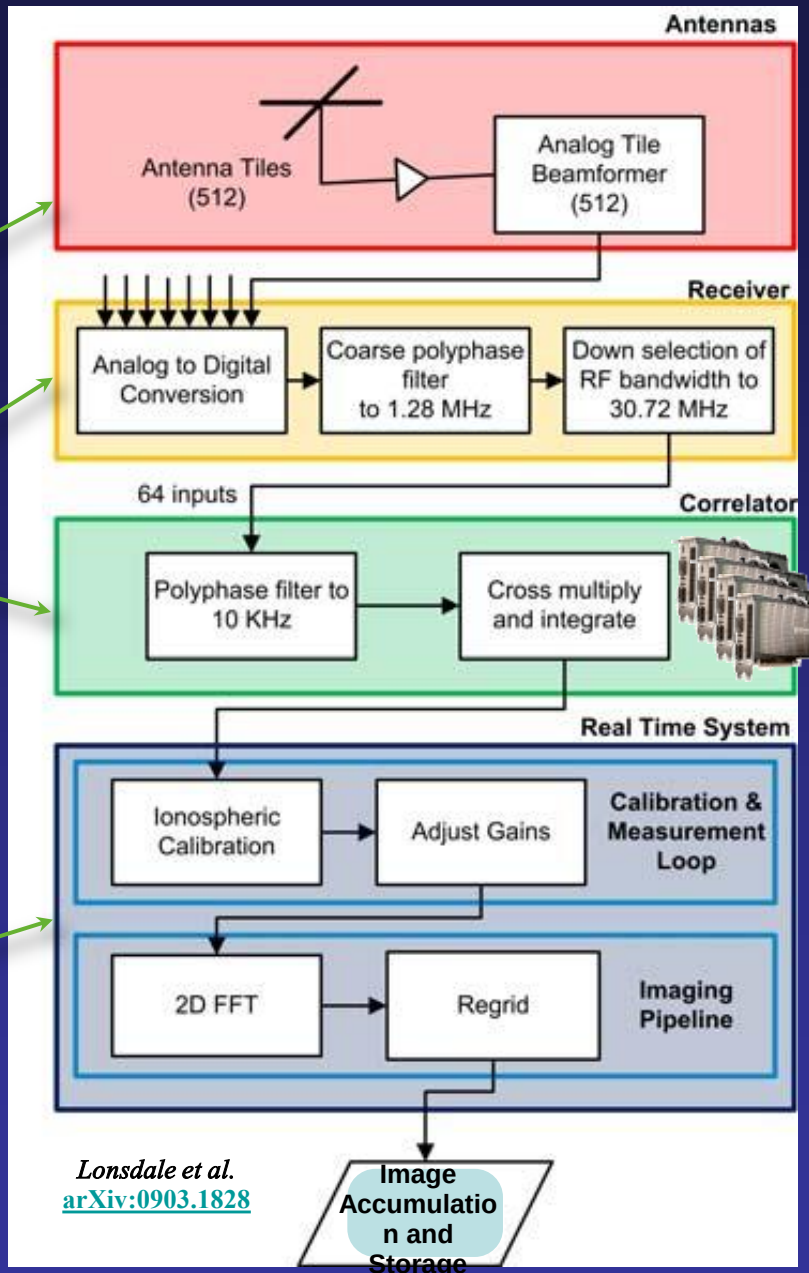

Correlator

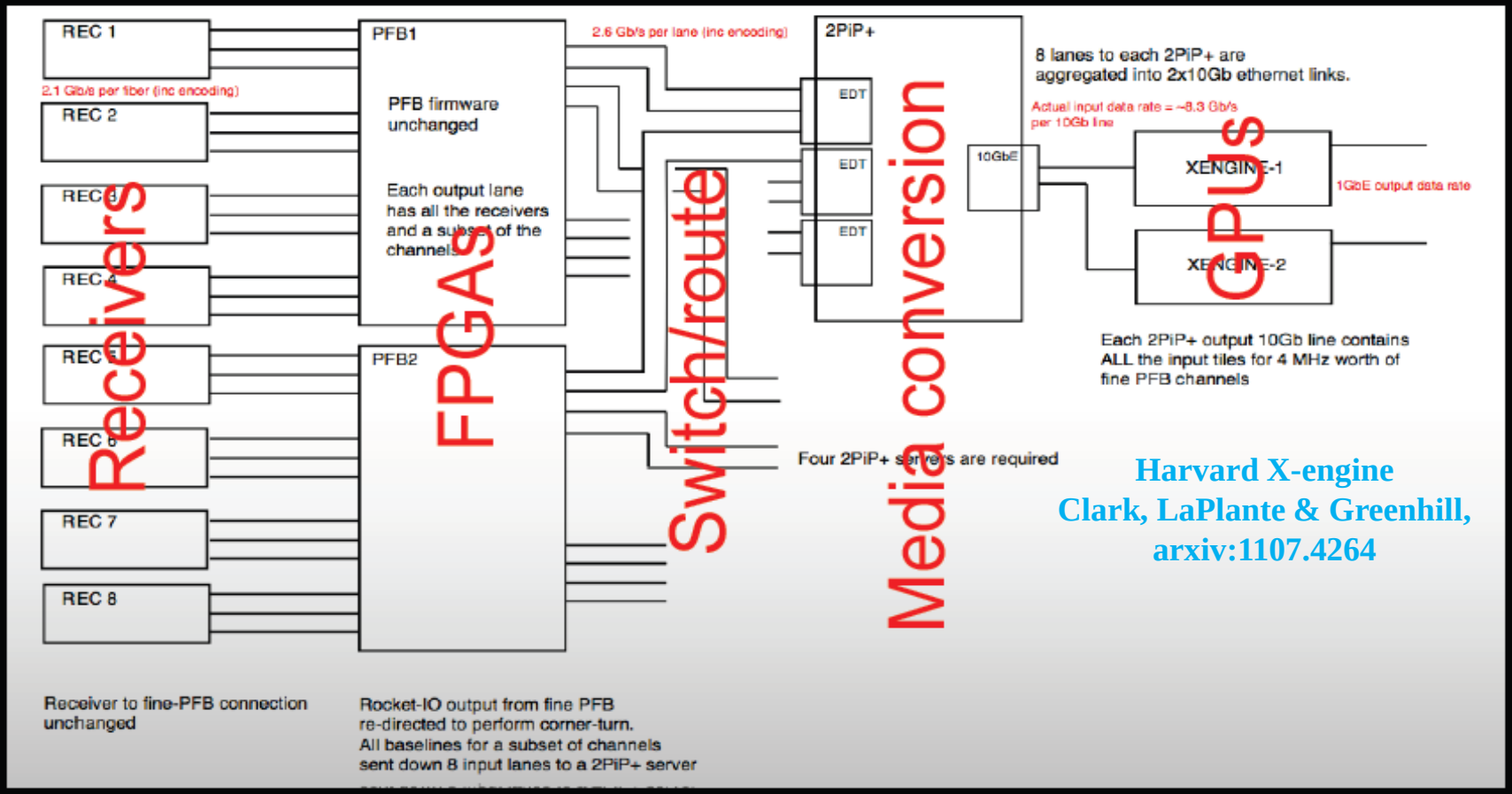

Stephen Ord

The Real-Time calibration and imaging System (RTS)

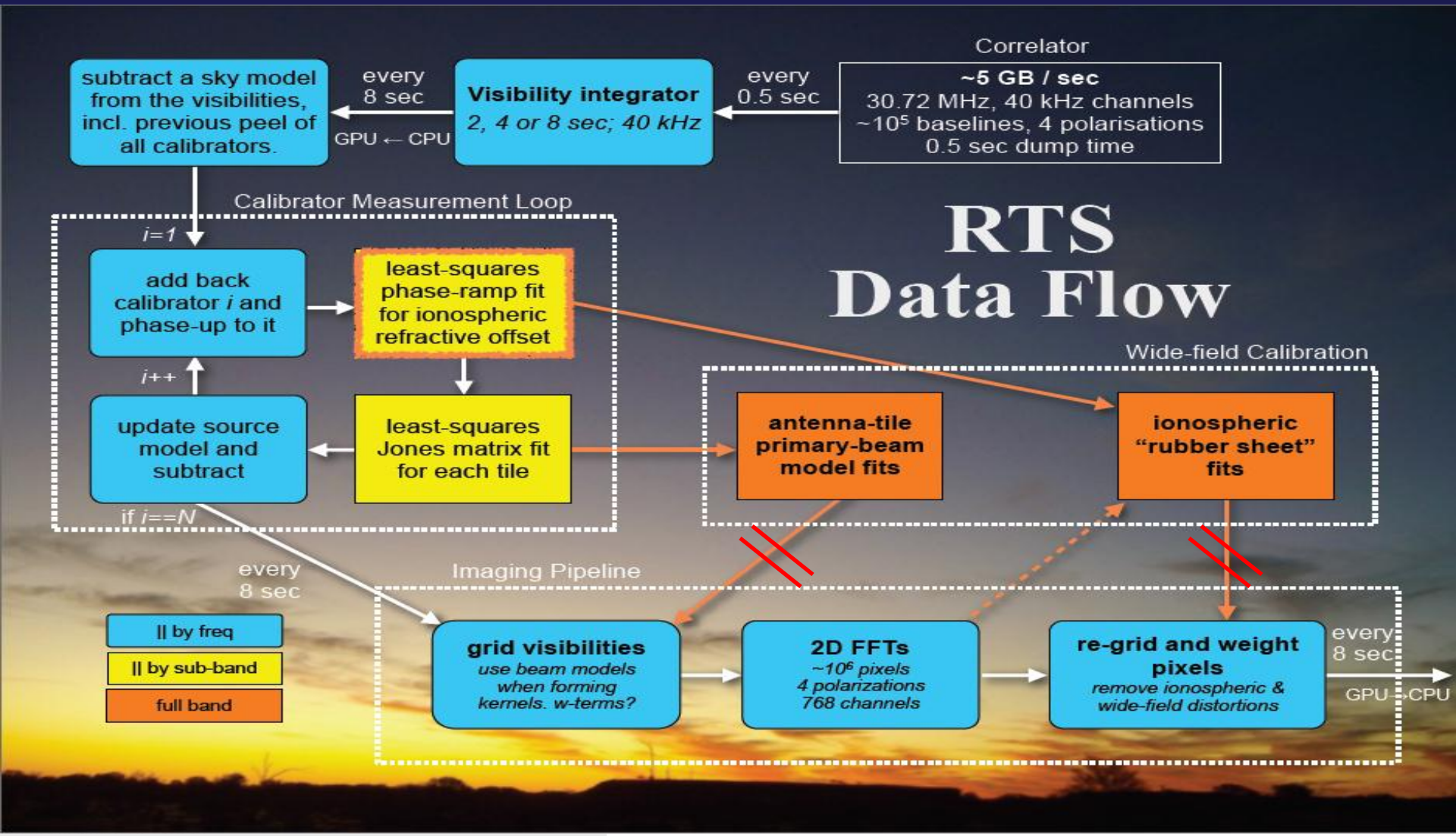

Calibration/hierarchical peeling:

- Use of point sources (so far) – 5 arcmin PSF
- Calibration-Measurement Loop (CML):
  - Source ranked based upon their apparent brightness (initial assumption of a tile beam);
  - Subtract an initial sky model;
  - Rotate and sum over frequency;
  - Estimate the ionospheric refraction through a λ^2 fit:

$$I'^{(K)}{}_{jk,c,f_0} \approx I_c - i2\pi(\alpha_c u_{jk,f_0} + \beta_c v_{jk,f_0})\,\lambda_0{}^2$$

(Mitchell et al., 2008, IEEE, 2, 707
Mitch = Oleg)

Calibration/hierarchical peeling (cont'd):

- Estimate the instrumental gain (global beam model):

$$I'^{(K)}{}_{jk,c,f_0} = \left(\sum_{k,k\neq j}^{N_\alpha} V_{jk,c,f_0}{}^{(K)} J_{k,c,f_0} \hat{P}_{c,f_0}{}^{\dagger} \right) \left(\sum_{k,k\neq j}^{N_\alpha} \hat{P}_{c,f_0} J_{k,c,f_0}{}^{\dagger} J_{k,c,f_0} \hat{P}_{c,f_0}{}^{\dagger} \right)^{-1}$$

No peeling

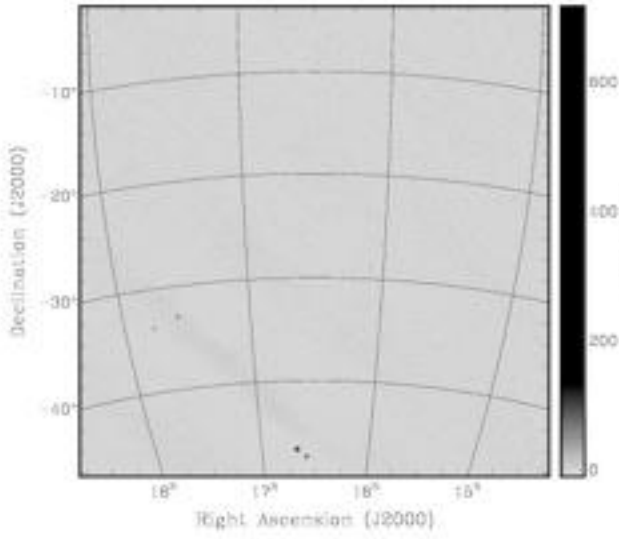

10 sources peeled

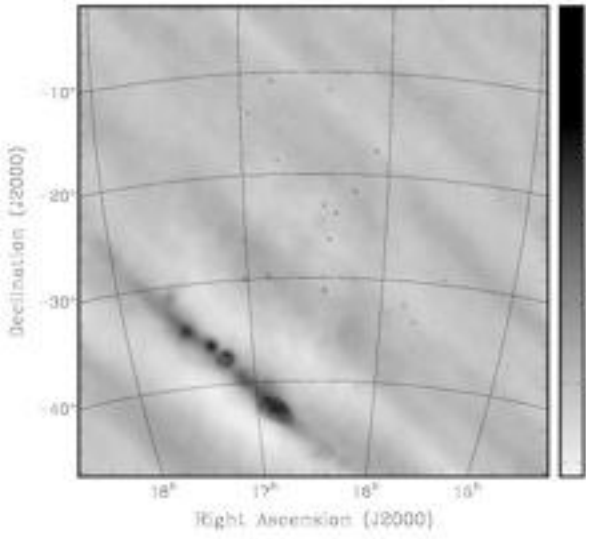

100 sources peeled

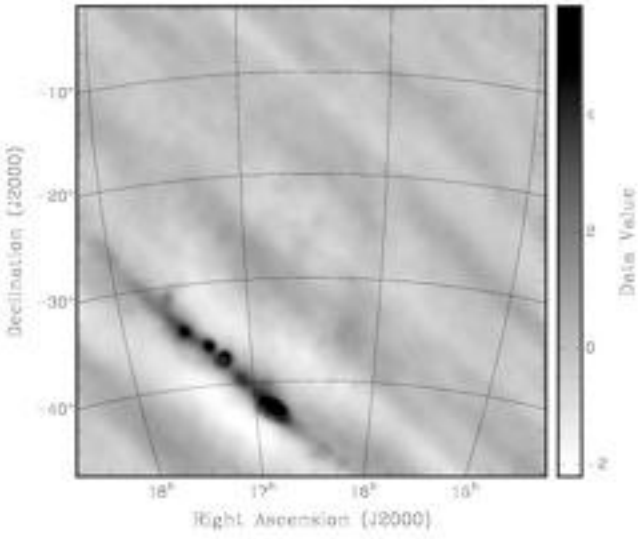

Imaging: warped snapshot imaging

- ***Imaging with dipole arrays is always mosaicking;***
- The array is instantaneously coplanar → 2D FFT
- Resample to a common reference frame → correction for a ionospheric refraction screen and for wide field effects in full polarization simultaneously;
- The time integration happens in the image plane, co-adding Healpix snapshot images

$$\widehat{\boldsymbol{b}}_{\boldsymbol{HPX}}{}^{\boldsymbol{S}} = \left[\left(\boldsymbol{J}_{\boldsymbol{pix}} \otimes \boldsymbol{J}_{\boldsymbol{pix}}\right)^{\dagger}\left(\boldsymbol{J}_{\boldsymbol{pix}} \otimes \boldsymbol{J}_{\boldsymbol{pix}}\right)\right]^{-1}\left(\boldsymbol{J}_{\boldsymbol{pix}} \otimes \boldsymbol{J}_{\boldsymbol{pix}}{}^{*}\right)^{\dagger}\left(\boldsymbol{J}_{\boldsymbol{true}} \otimes \boldsymbol{J}_{\boldsymbol{true}}{}^{*}\right)\boldsymbol{S}\boldsymbol{b}_{\boldsymbol{HPX}}{}^{\boldsymbol{S}}$$

- Integration in the image domain is easily parallelizable in time and frequency → achieved real time processing for the MWA 32T data;

(Ord et al., 2010, PASP, 122, 1353)

Iterative deconvolution/source subtraction via forward modeling
(image based deconvolution)

(Pindor et al., 2011, PASA, 28, 46)
(Bernardi et al., 2011, MNRAS, 413, 411)

- when the MWA works in real time mode, visibility data are not stored – causing a possible limitation in the deconvolution accuracy;
- once the uv plane includes corrections for time and position dependent primary (different from each other) and ionospheric distorsions the PSF is position dependent → no standard deconvolution method applicable (no Clean, no Cotton-Schwab method);
- This method does not alter the statistics of the residual visibilities (important for EoR);

Flow chart

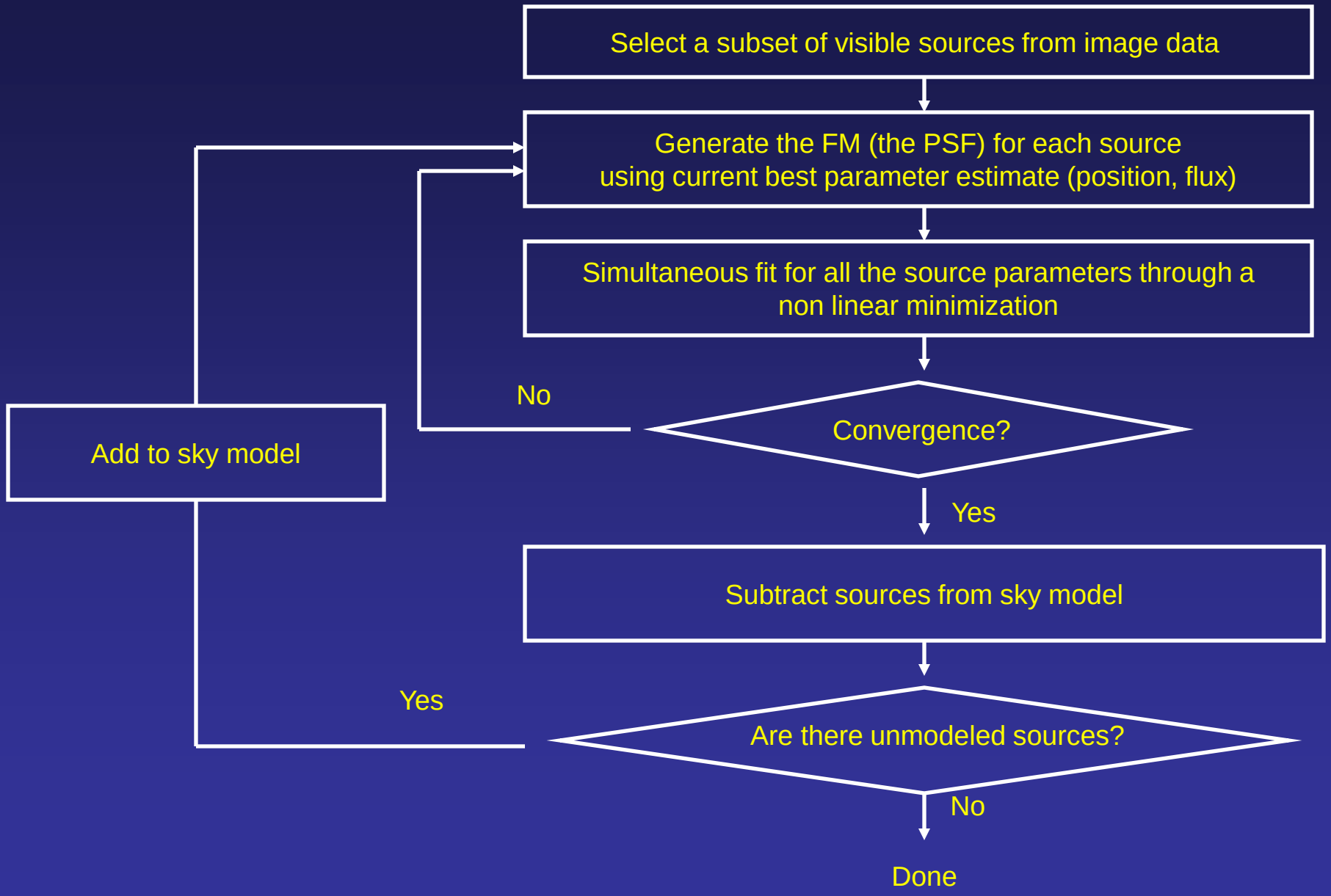
Select a subset of visible sources from image data
Generate the FM (the PSF) for each source
using current best parameter estimate (position, flux)
Simultaneous fit for all the source parameters through a
non linear minimization
Convergence?
No
Yes
Add to sky model
Subtract sources from sky model
Are there unmodeled sources?
Yes
No
Done

Deconvolution can be represented by matrix algebra:

- for M sources and N image pixels, the following system of linearized equations is solved at each iteration:

$$\delta x = (J^T W J)^{-1} J^T W \delta m$$

3M vector of parameter estimates — δx

Jacobian matrix — J

weight matrix — W

N vector of data points — δm

- get a new parameter estimate $x_{i:}$

$$x_i = x_{i-1} - \delta x$$

MWA 32 tiles (32T)

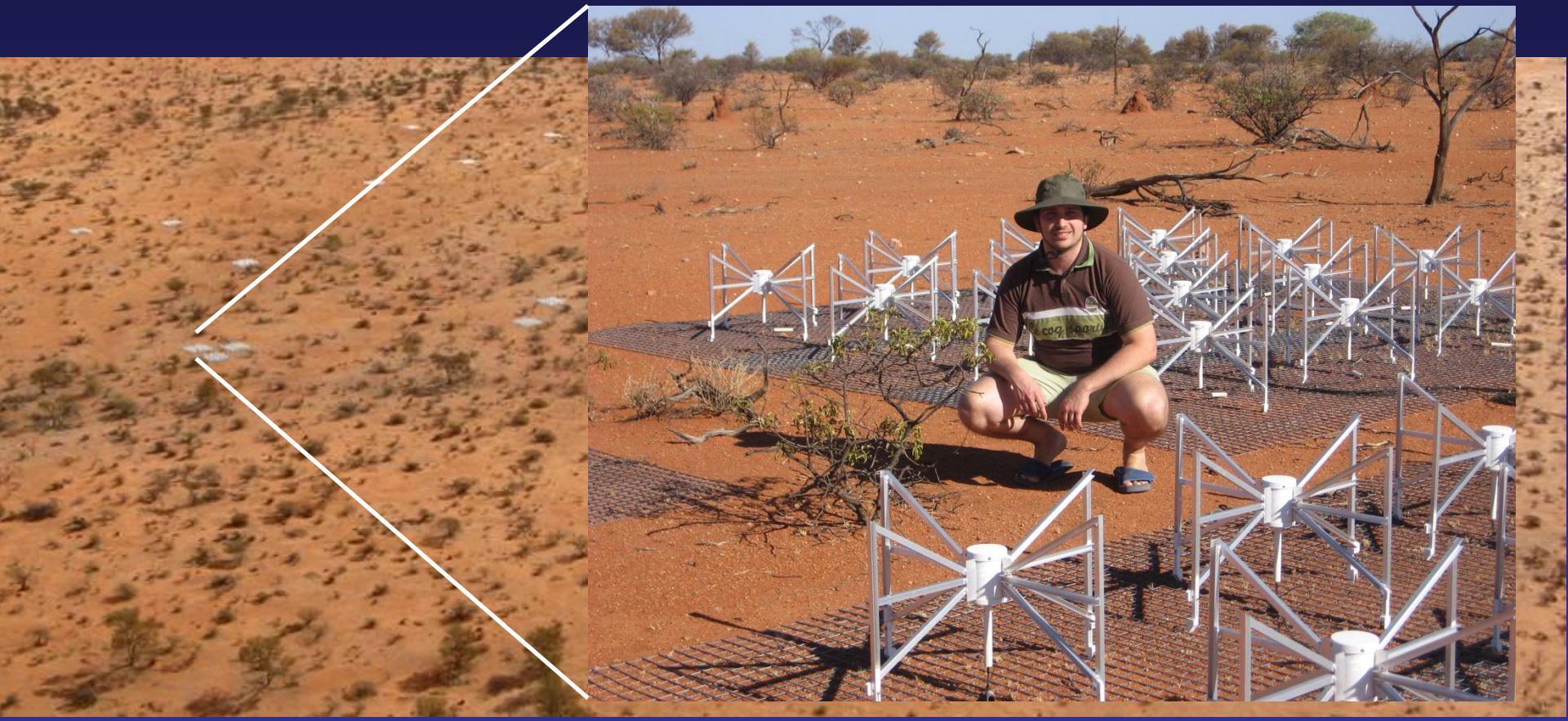

…5% prototype

MWA 32T calibration and imaging

- polynomial fit to the bandpass towards the brightest source;
- bandpass applied in a direction independent fashion;
- correction for DDEs are possible for CAT I sources (a handful for the 32T sensitivity);
- imaging assumes that the tile beams are all the same;
- image deconvolution via forward modeling for CAT II sources (propagation of the sky models through the calibration and imaging pipeline → accounting for direction dependent PSF – which is always the case for dipole arrays);

Primary beam measurements

- the sky drifts overhead while the tiles keep pointing at zenith;
- 30.72 MHz bandwidth centered @ 188.8 MHz;
- snapshot images (one every 5 min) are used to measure the beam response towards J0444-2905 (which is ~ 44.5 Jy @ 160 MHz – tied to the Baars scale);
- simple tile beam model based on the co-addition of 16 dipole beams:

$$dp = 2\sin(2\pi d_h \cos(za))\sqrt{1-[\sin(za)\cos(az)]^2}$$

Primary beam measurements (cont'd)

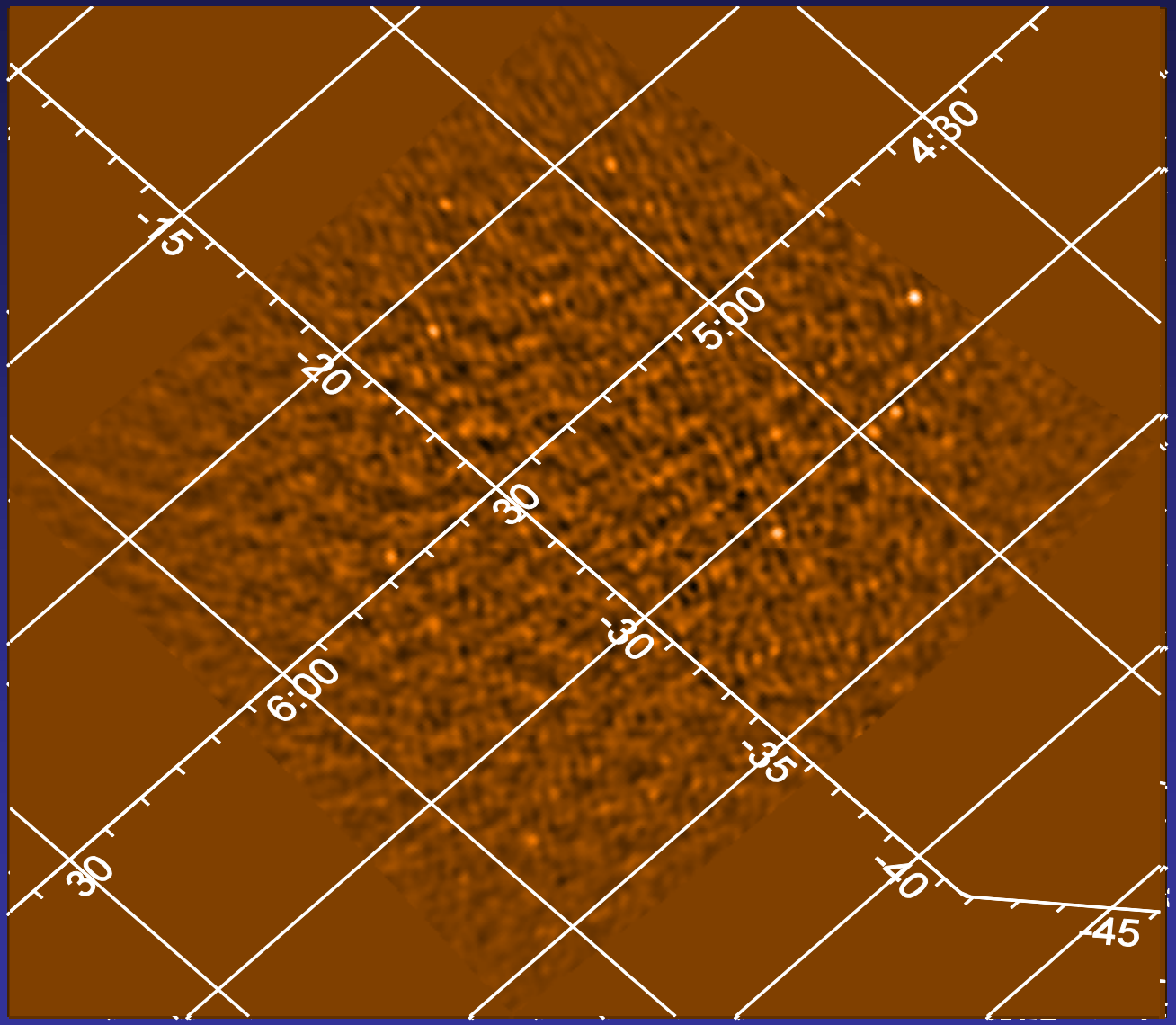

Primary beam measurements (cont'd)

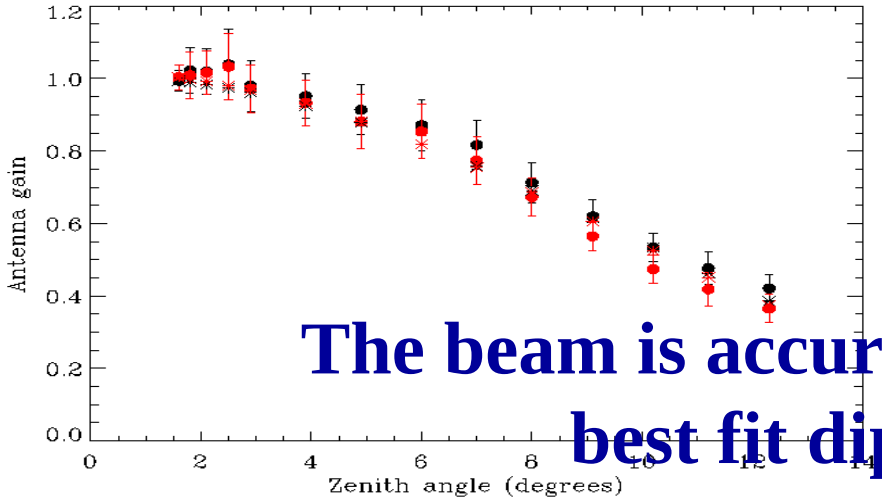

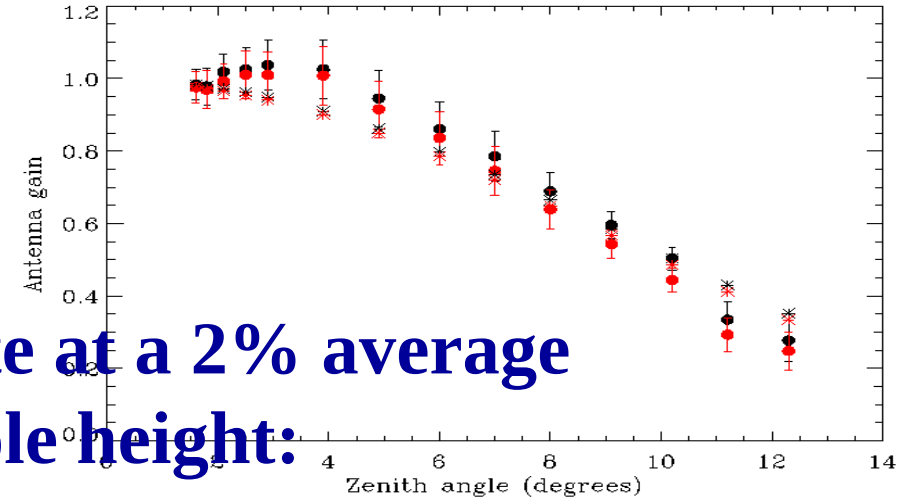

The beam is accurate at a 2% average

best fit dipole height:

d_h: (0.33 ± 0.06) m

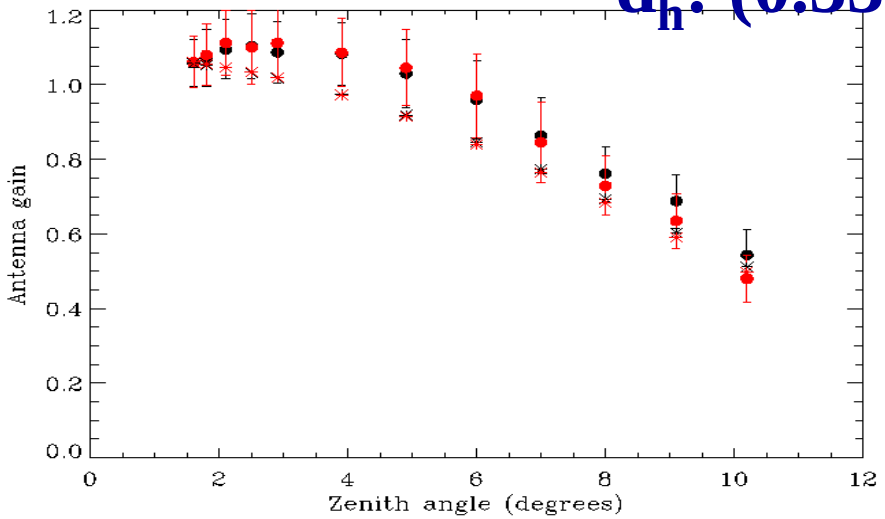

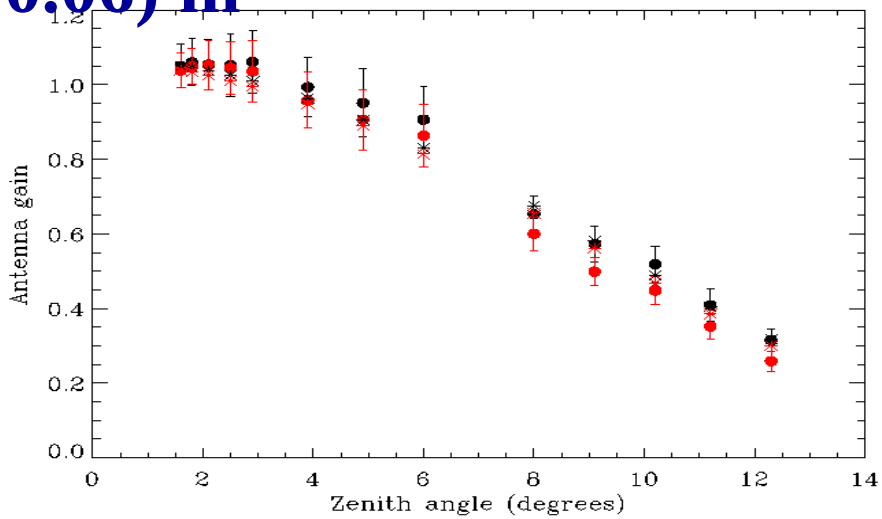

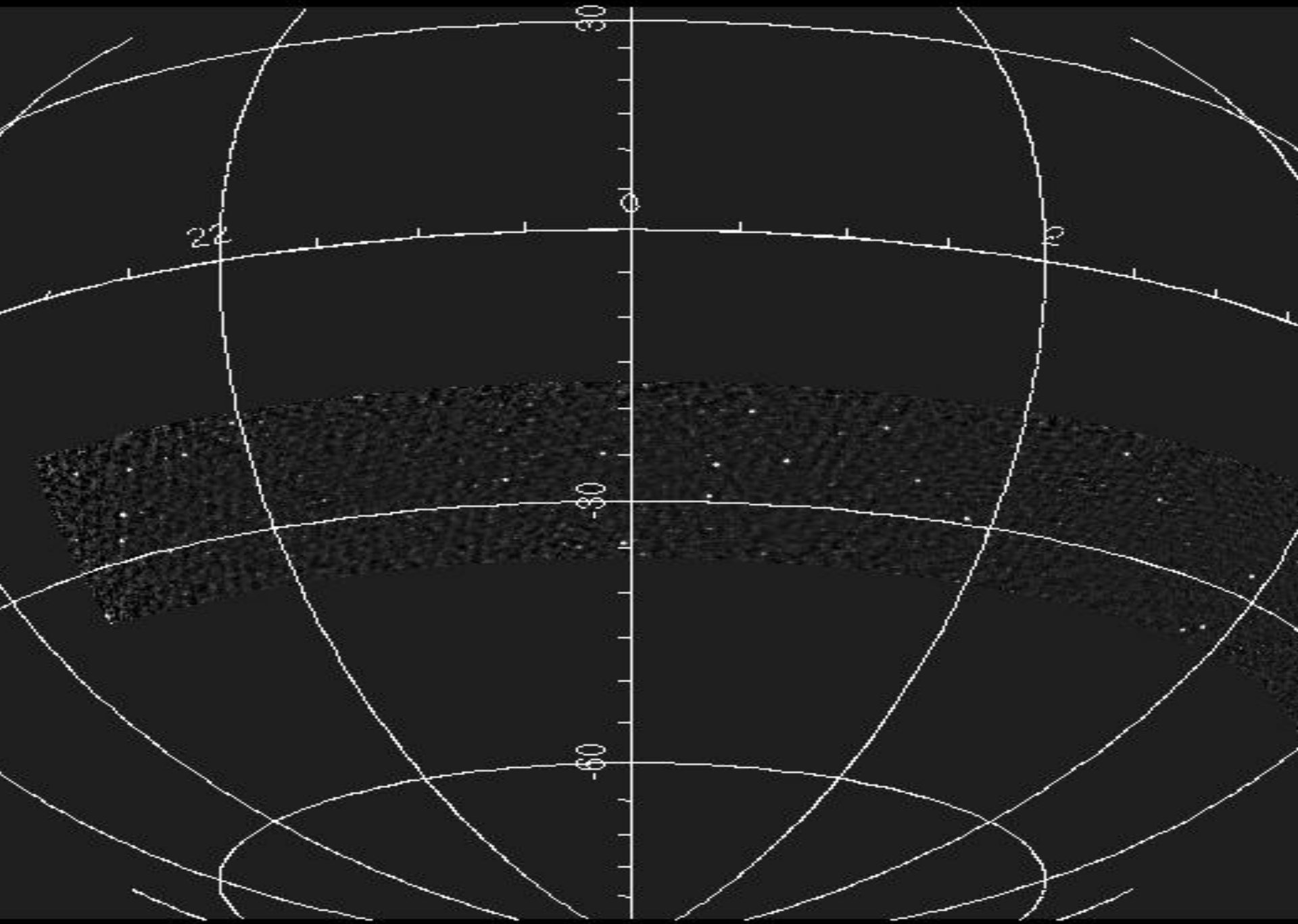
30
0
22
8
-30
-60
Right ascension

Primary beam calibrated drift-scan sky survey:

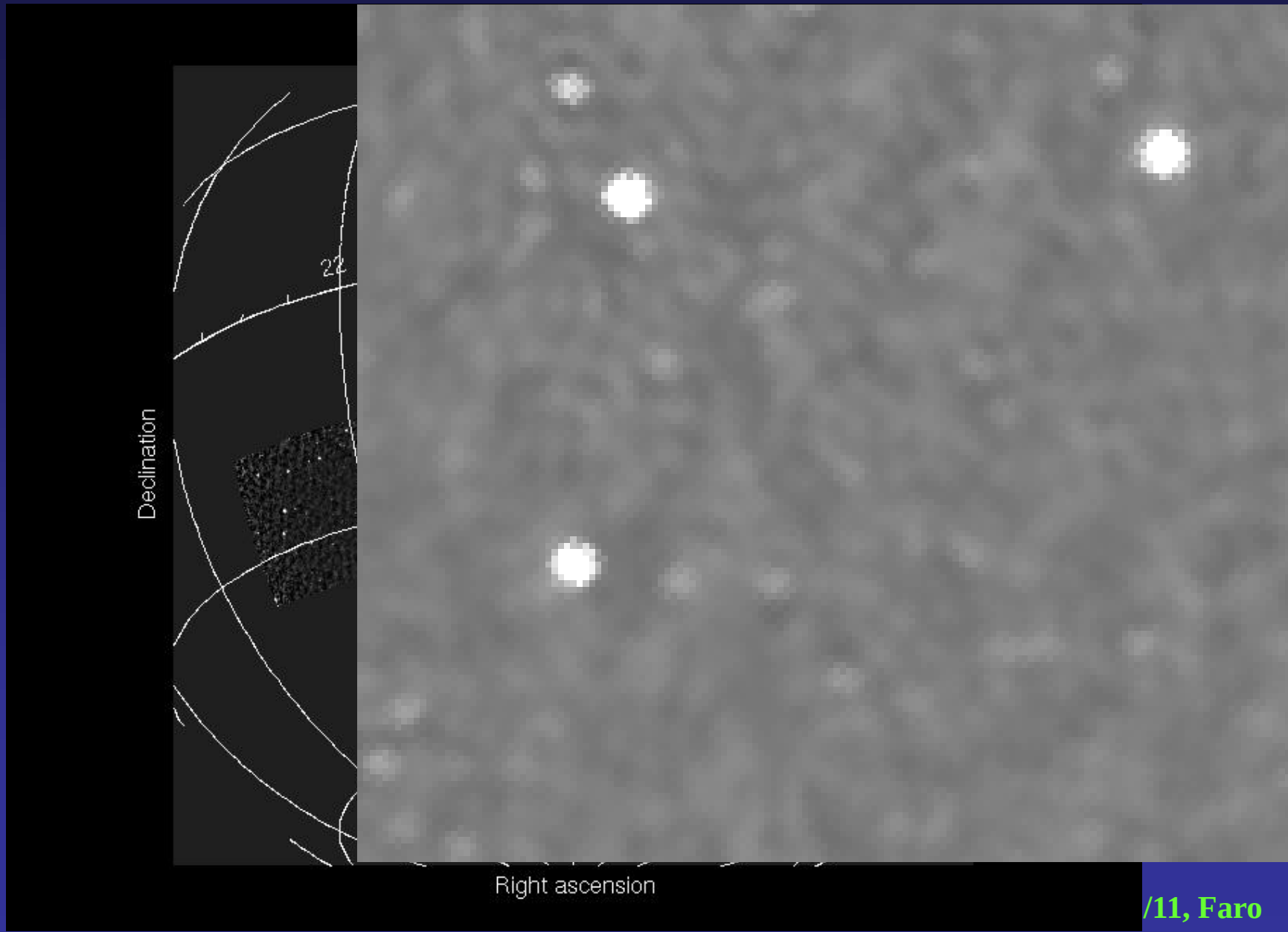

Primary beam calibrated drift-scan sky survey:

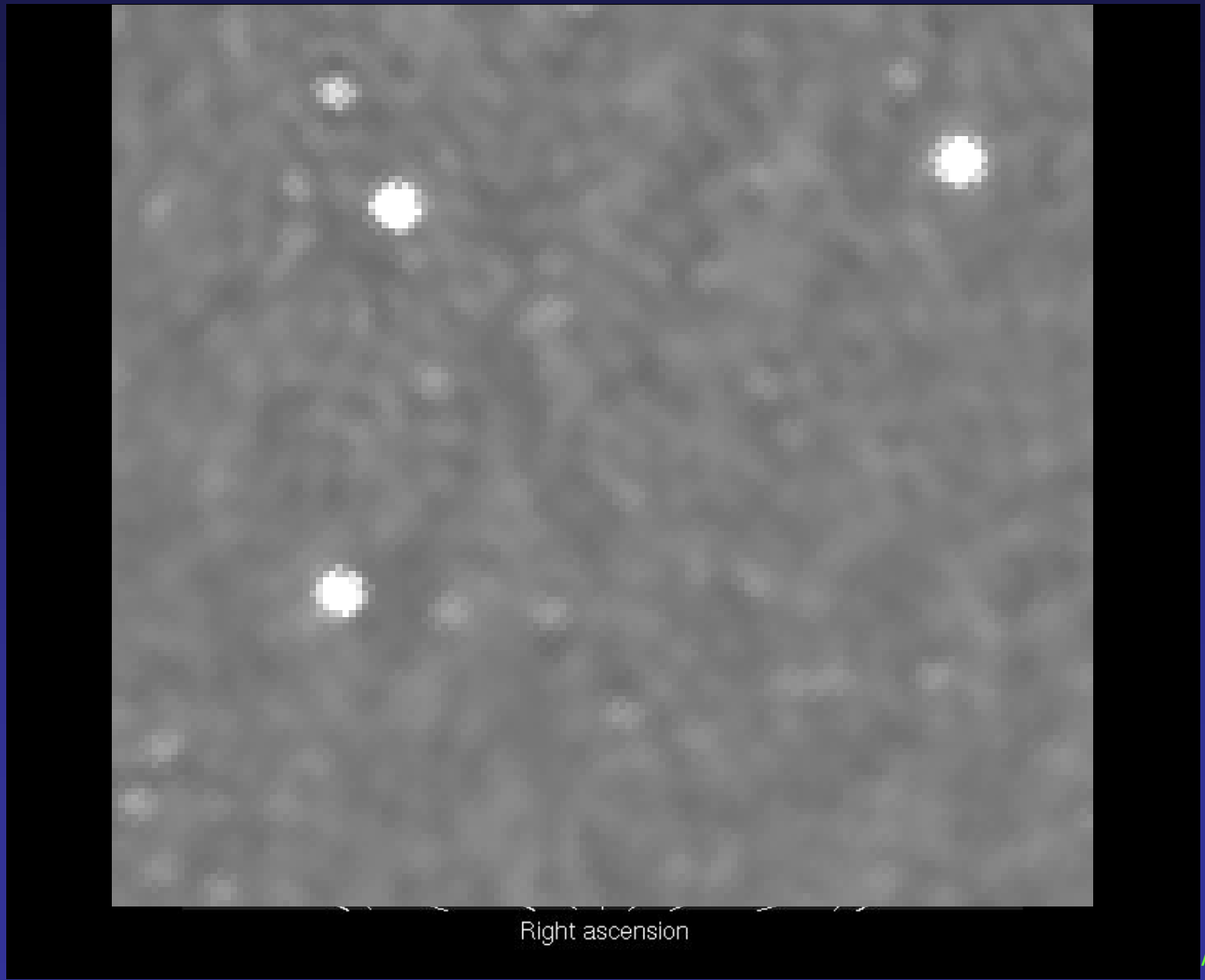

Primary beam calibrated drift-scan sky survey:

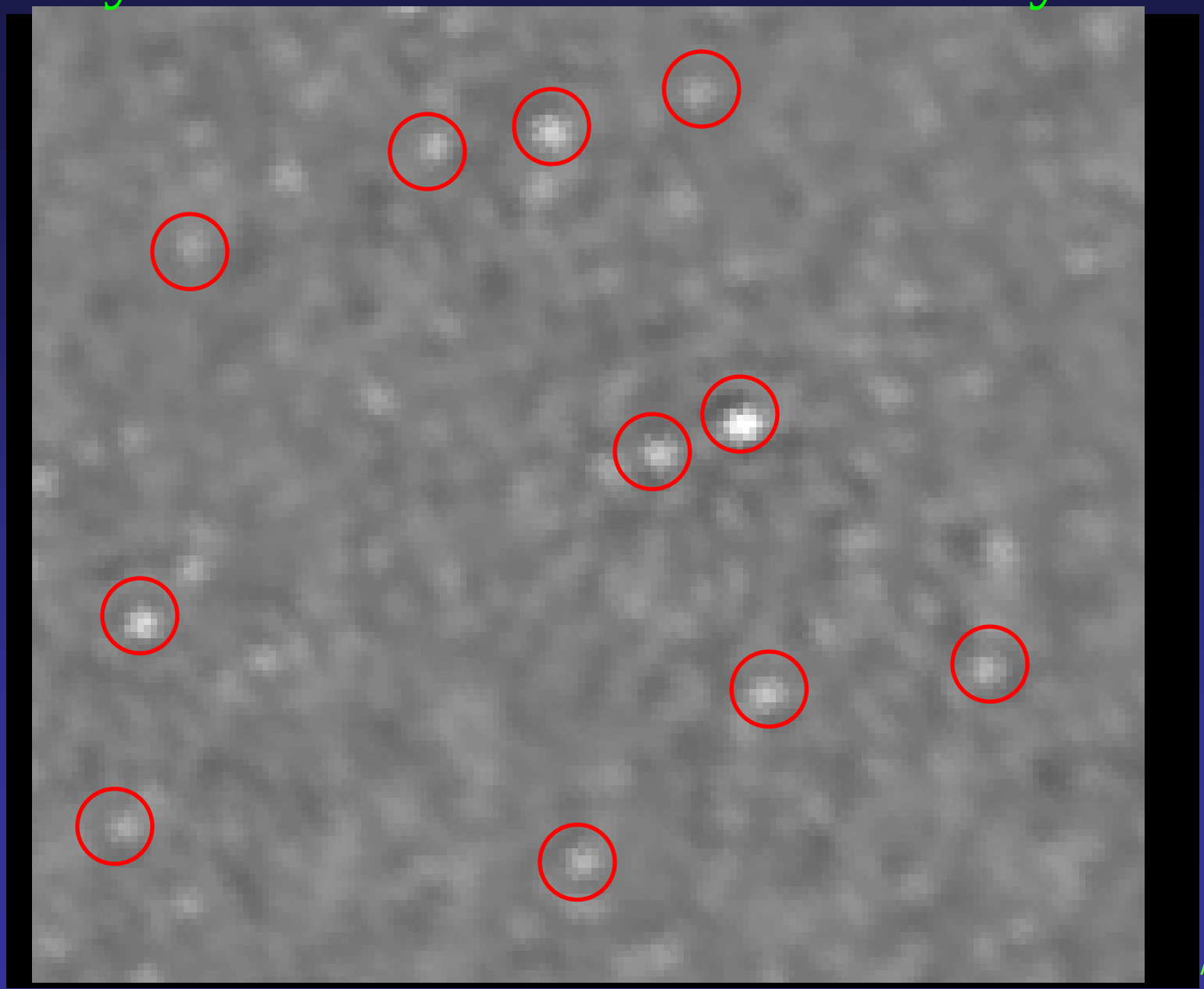

Primary beam calibrated drift-scan sky survey: out of beam sources

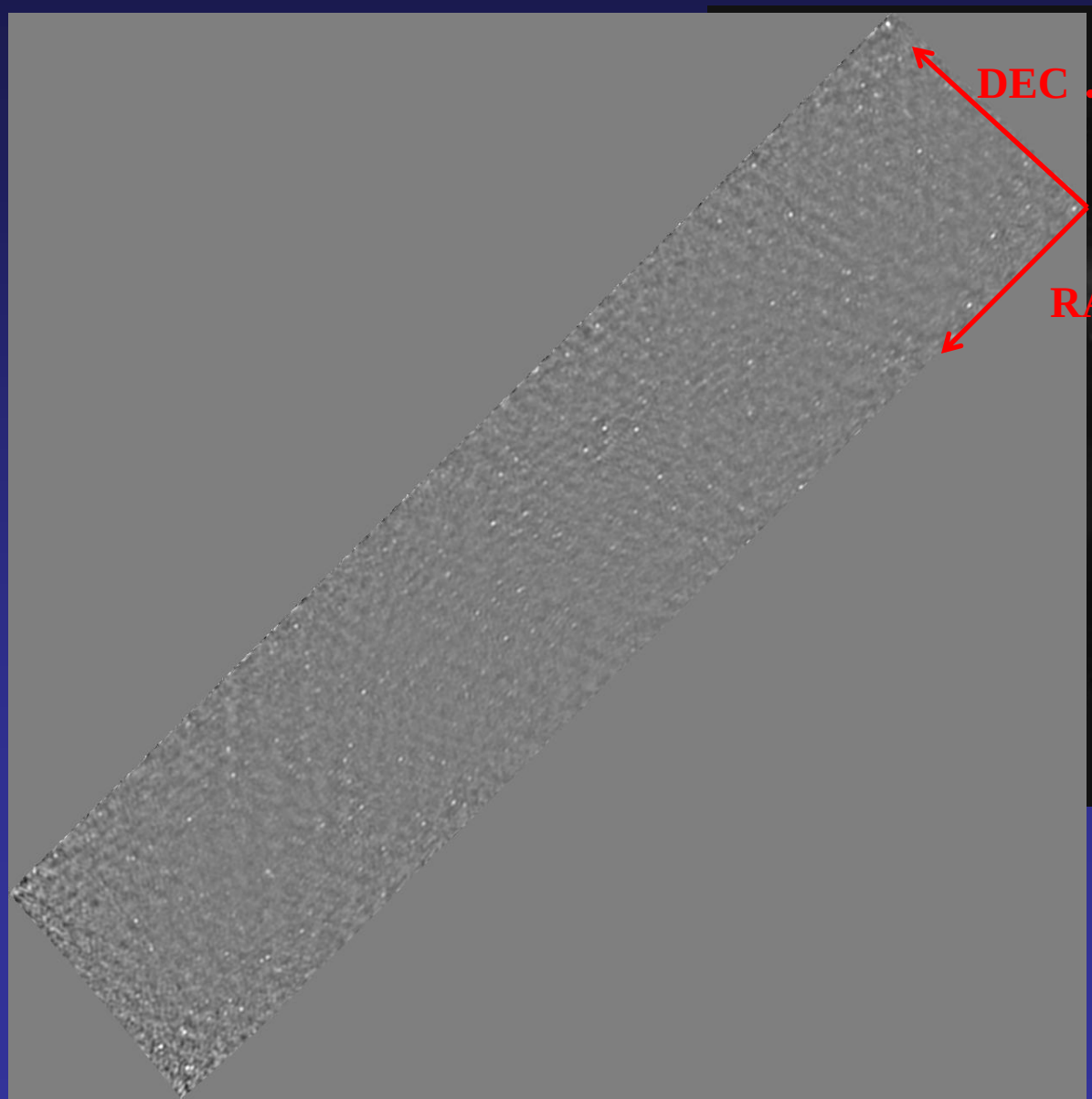

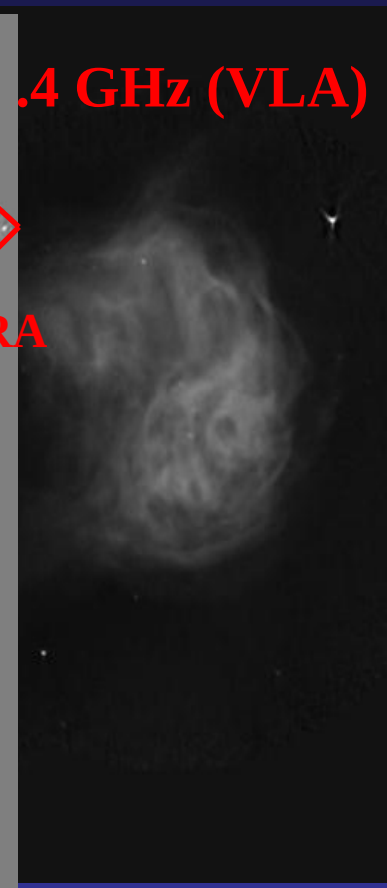

First calibrated image of ForA @ < 200 MHz, with 15’ resolution

Integrated flux @ 188.8 MHz ~ 510 Jy

$\alpha_{1421\text{-}188.8} = 0.71$

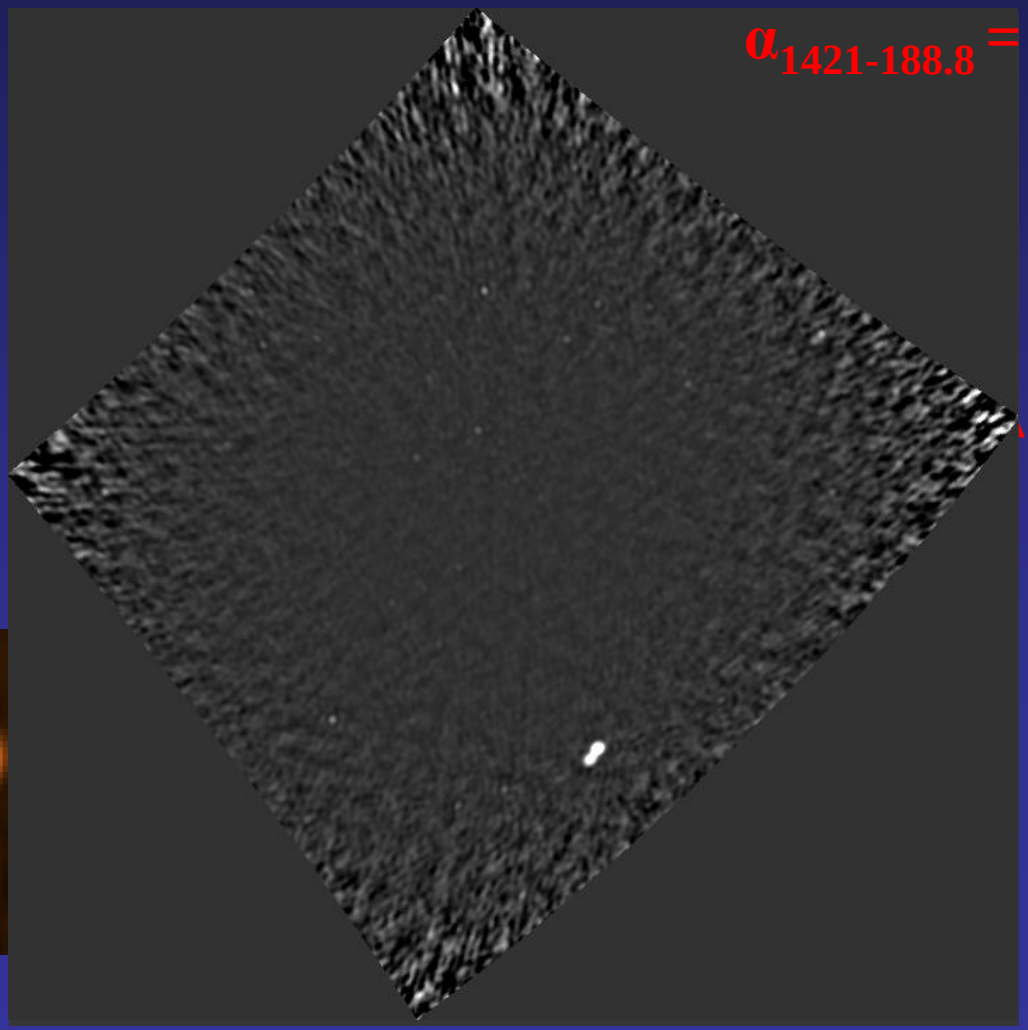

Wide field polarimetry: Stokes Q

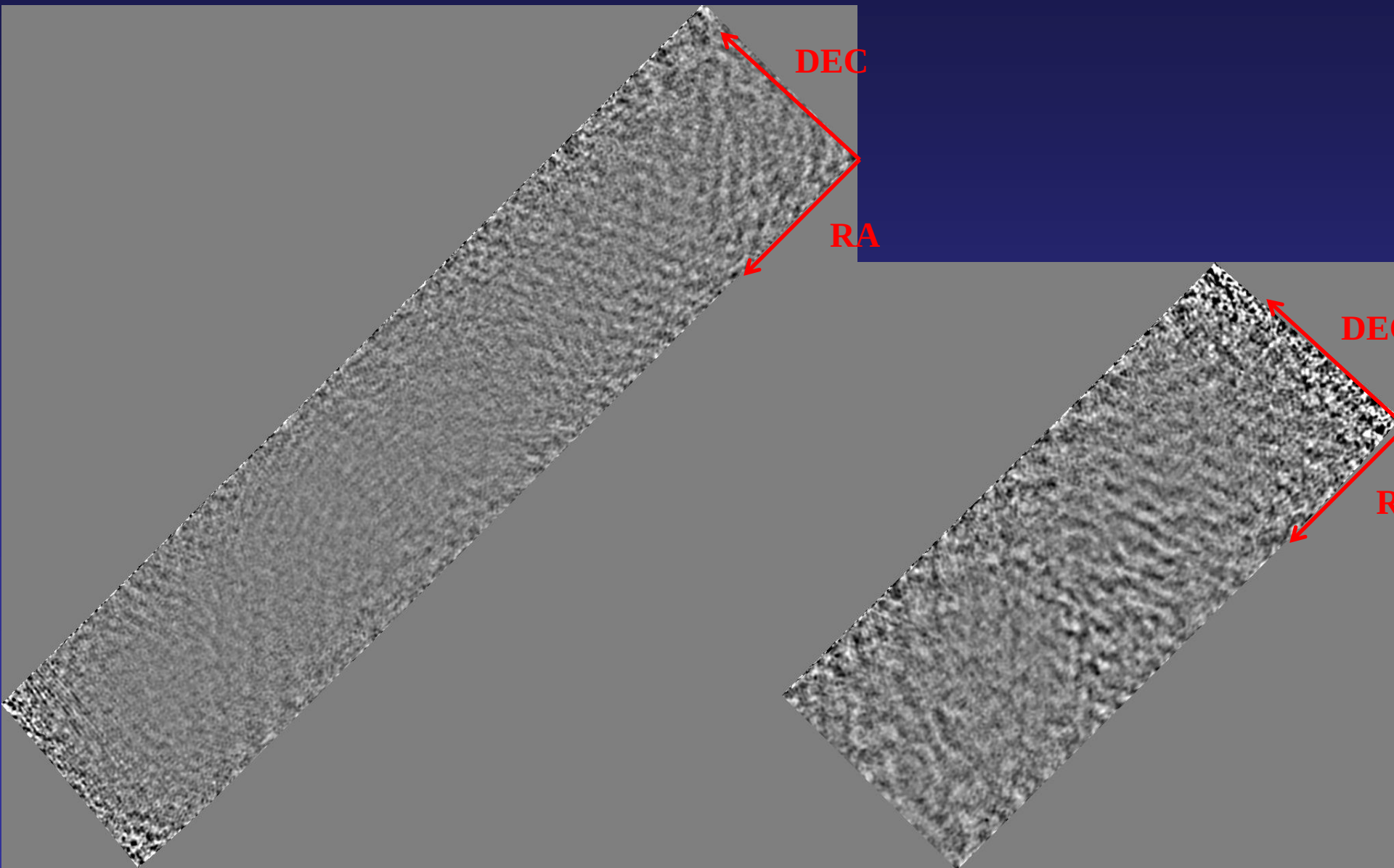

Wide field polarimetry: Stokes U

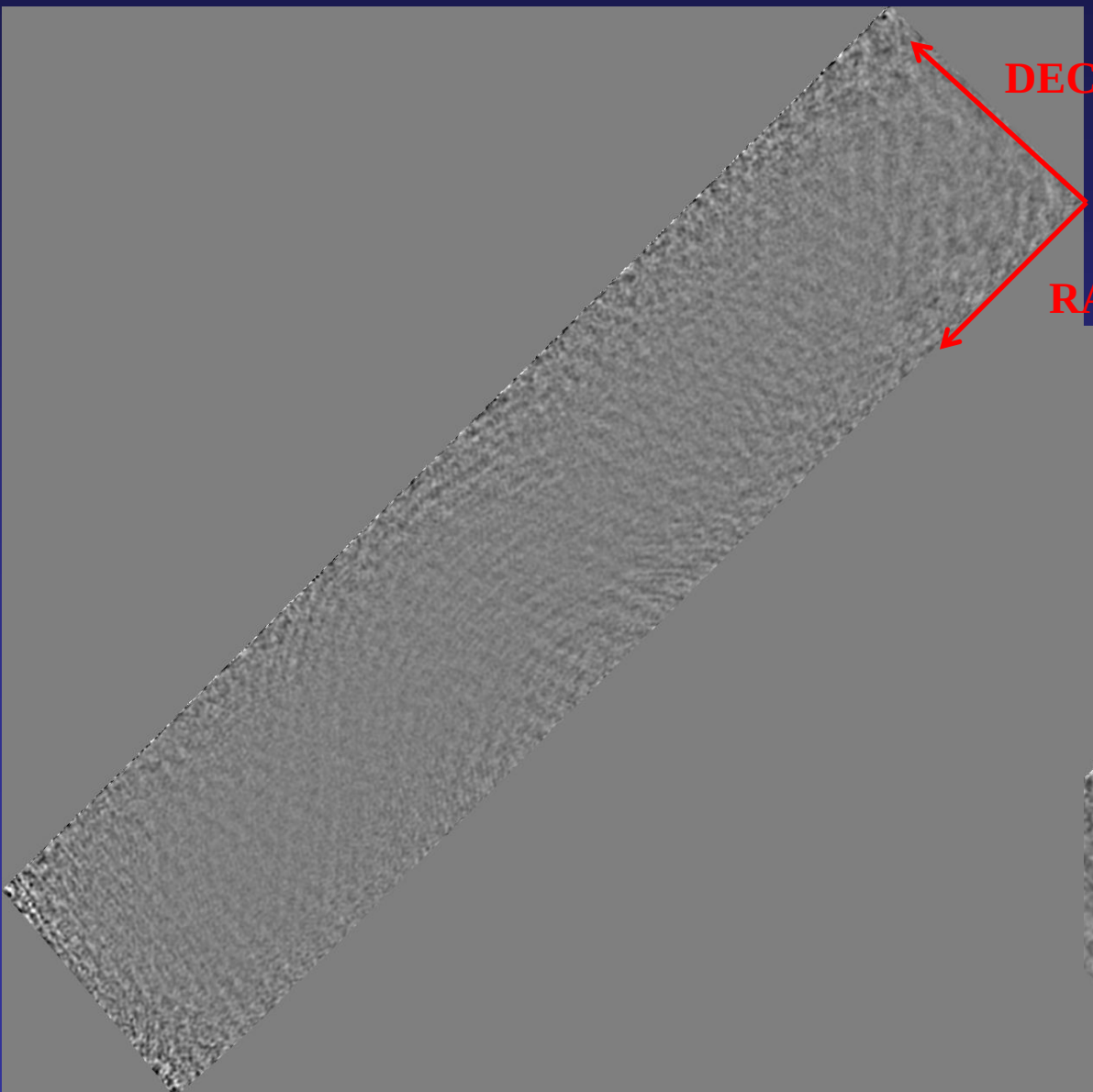

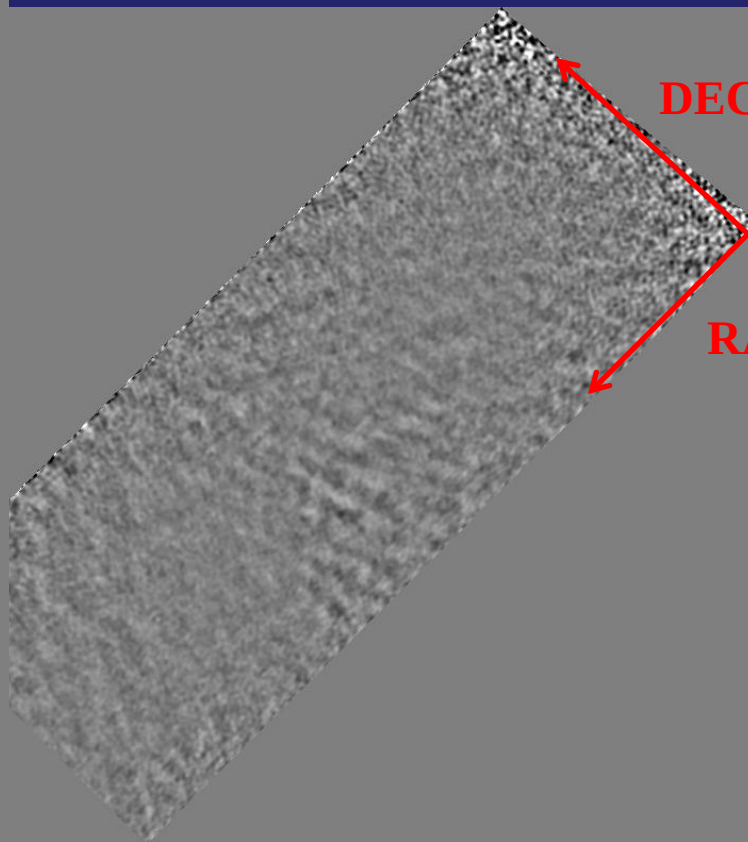

Forward modeling example

Residual image (→ DDEs, 4th GC)

Keeping in mind that the 32T array is not for high dynamic range…

~ 90 sources subtracted (~ real time processing)

Residual: rms ~ 0.4 Jy/beam on Stokes I, ~ 0.02 Jy/beam on Stokes U

Limited by confusion from sky sources and sidelobes

Dynamic range ~ 8000; actual dynamic range ~ 400

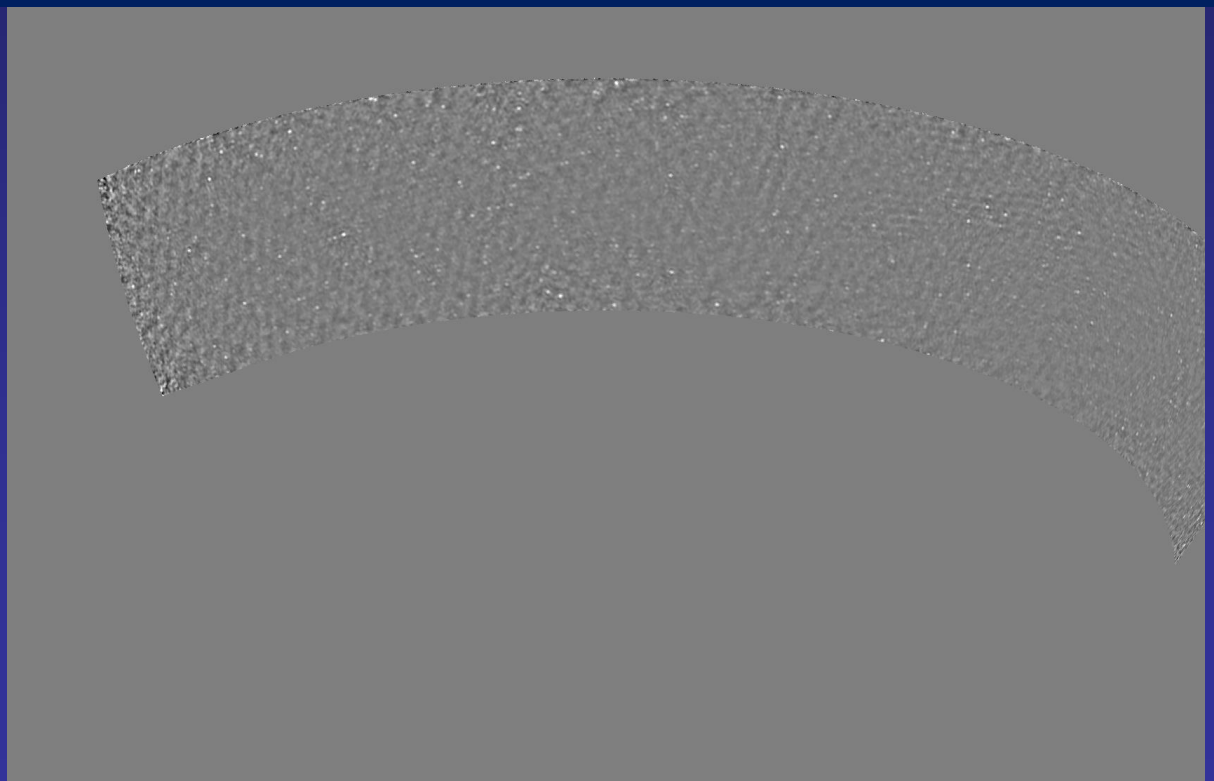

Most important (to me): calibration is ready to deliver real science…

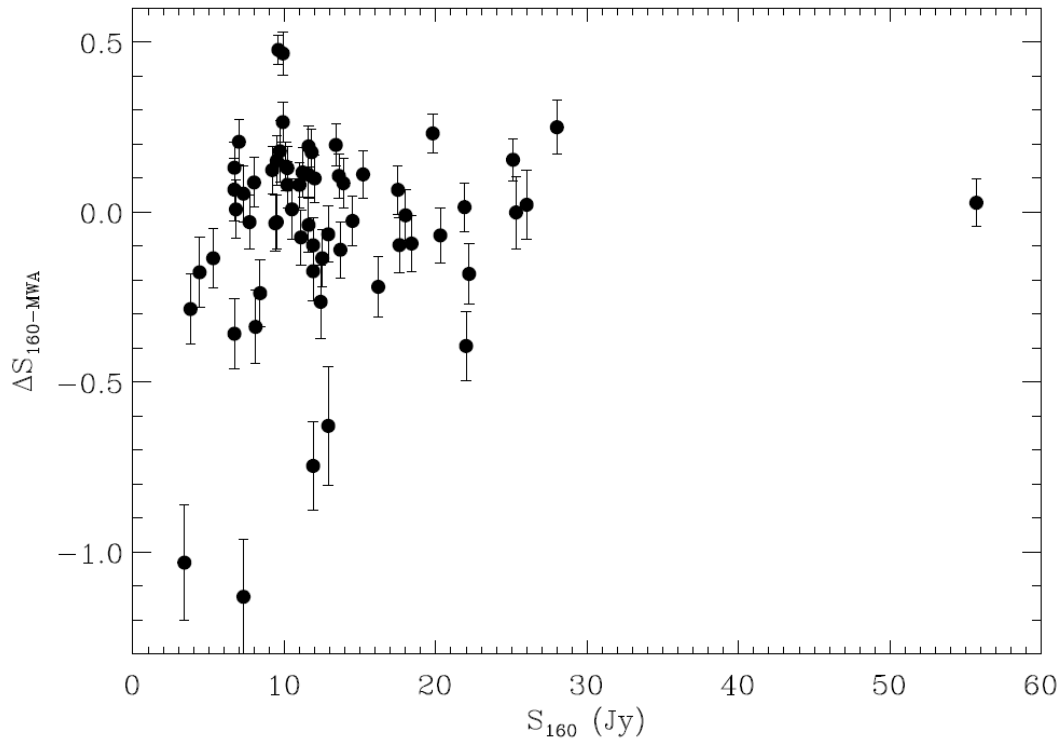

Comparison between the first 60 brightest MWA sources (down to ~ a few Jy) matched with the Culgoora measurements (160 MHz, 3.5' resolution, Slee 1988)

15% rms scatter

… cont'd

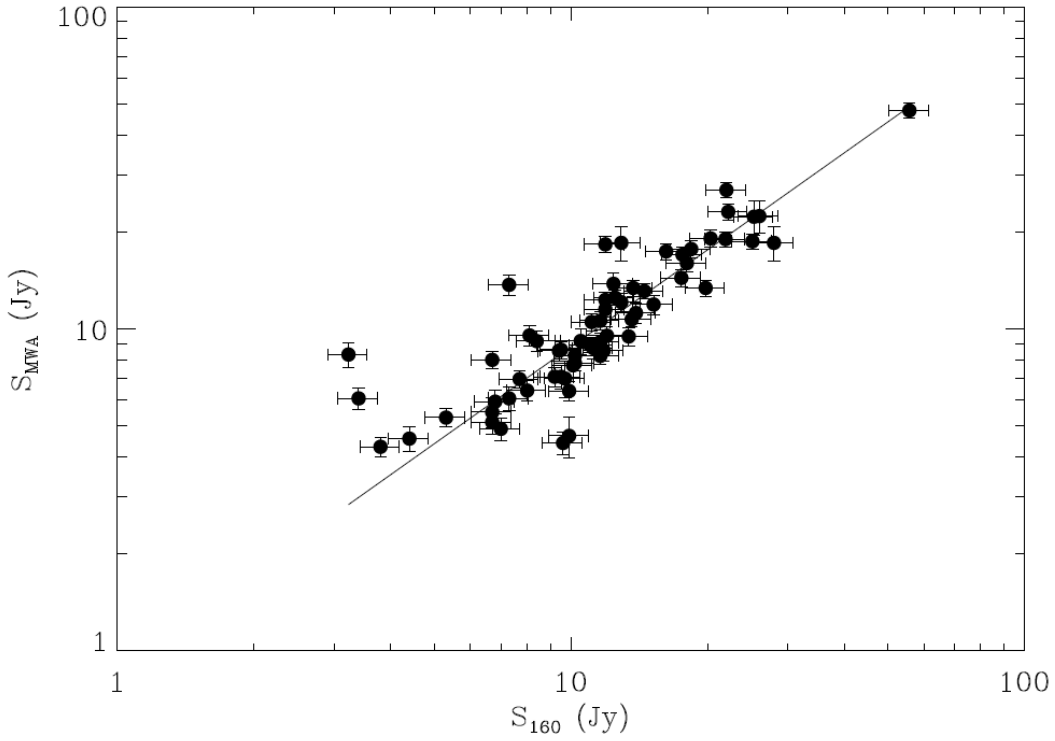

Best fit spectral index among the two source measurements: 0.77 ± 0.18

Conclusions:

- Successful tests of the MWA CPU/GPU calibration-imaging-deconvolution pipeline – but people will keep working on it;
- First attempt to model tile beams over the full bandwdith → successful but still very limited in applications;
- Drift scan tech[illegible] disentangle the sky model/primary beam degeneracy → more to come in the current expedition on site;
- First full-polarimetric large-area (~2700 square degrees) MWA survey (sources down to a few Jy, first low frequency image of ForA)
- Next MWA stop is 128T;

Thank you!